
Sim and Real: Better Together

Shirli Di Castro Shashua *
Technion Institute of Technology
Haifa, Israel

Dotan Di Castro
Bosch Center of AI
Haifa, Israel

Shie Mannor
Technion Institute of Technology
Haifa, Israel

Abstract

Simulation is used extensively in autonomous systems, particularly in robotic manipulation. By far, the most common approach is to train a controller in simulation, and then use it as an initial starting point for the real system. We demonstrate how to learn simultaneously from both simulation and interaction with the real environment. We propose an algorithm for balancing the large number of samples from the high throughput but less accurate simulation and the low-throughput, high-fidelity and costly samples from the real environment. We achieve that by maintaining a replay buffer for each environment the agent interacts with. We analyze such multi-environment interaction theoretically, and provide convergence properties, through a novel theoretical replay buffer analysis. We demonstrate the efficacy of our method on a sim-to-real environment.

1 Introduction

Reinforcement learning (RL) is a framework where an agent interacts with an unknown environment, receives a feedback from it, and optimizes its performance accordingly [45, 3]. There have been attempts of learning a control policy directly from real world samples [29, 50, 37, 22]. However, in many cases, learning from the actual environment may be slow, costly, or dangerous, while learning from a simulated system can be fast, cheap, and safe. The advantages of learning from simulation are counterbalanced by the *reality-gap* [19]: the loss of fidelity due to modeling limitations, parameter errors, and lack of variety in physical properties. The quality of the simulation may vary: when the simulation mimics the reality well, we can train the agent on the simulation and then transfer the policy to the real environment, in a one shot manner (e.g., [2]). However in many cases, simulation demonstrates low fidelity which leads to the following question: *Can we mitigate the differences between real environments ("real") and simulations ("sim") thereof, so as to train an agent that learns from both, and performs well in the real one?*

In this work, we propose to learn simultaneously on real and sim, while controlling the rate in which we collect samples from each environment and controlling the rate in which we use these samples in the policy optimization. This synergy offers a speed-fidelity trade-off and harnesses the advantage of each domain. Moreover, the simulation speed encourages exploration that helps to accelerate the learning process. The real system in turn can improve exploitation in the sense that it mitigates the challenges of sim-to-real policy transfer, and encourages the learner to converge to relevant solutions. A general scheme describing our proposed setup is depicted in Figure 1. In a nutshell, there is a single agent interacting with K environments (on the left). Each sample provided by an environment is pushed into a corresponding replay buffer (RB). On the right, the agent pulls samples from the RBs and is trained on them. In the sim-to-real scheme, $K = 2$.

*This research was conducted during an internship in Bosch Center of AI.

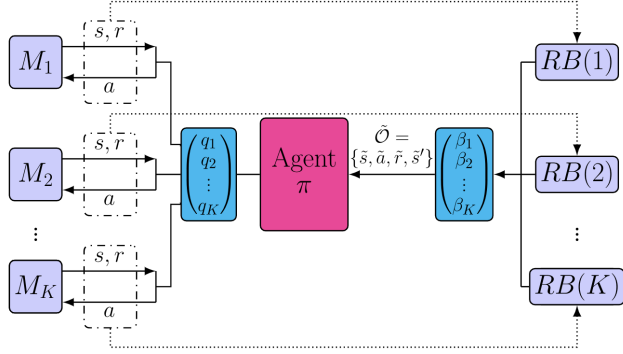


Figure 1: Mixing K environments scheme. The agent selects an environment M_i with probability q_i and interacts with it. Simultaneously, the agent chooses $RB(j)$ with probability β_j and samples from this replay buffer a stored transition \hat{O} , which is used for estimating the TD error and update the policy parameters.

In the specific scheme for mixing real and sim samples in the learning process, separate probability measures for collecting samples and for optimizing parameters policies are used. The off-policy nature of our scheme enables separation between real and sim samples which in turn helps controlling the rate of real samples used in the optimization process. In this work we discuss two RL algorithms that can be used with this scheme: (1) off-policy linear actor critic with mixing sim and real samples and (2) Deep Deterministic Policy Gradient (DDPG; [30]) mixing scheme variant based on neural networks. We analyze the asymptotic convergence of the linear algorithm and demonstrate the mixing samples variant of DDPG in a sim-to-real environment.

The naive approach in which one pushes the state-action-reward-next-state tuples into a single shared replay buffer is prone to failures due to the imbalance between simulation and real roll-outs. To overcome this, we maintain separate replay buffers for each of the environments (e.g., in the case of a single robot and a simulator we would have two replay buffers). This allows us to extract the maximum valuable information from reality by distinguishing its tuples from those generated by other environments, while continuously improving the agent using data from all input streams. Importantly, although the rate of samples is skewed in favor of the simulation, the learning may be carried out using a different rate. In a sense, the mechanism we suggest is a version of the *importance sampling* technique [11].

Our main contributions in this work are as follows:

1. We present a method for incorporating real system samples and simulation samples in a policy optimization process while distinguishing between the rate of collecting samples and the rate of using them.
2. We analyze the asymptotic convergence of our proposed mixing real and sim scheme.
3. To the best of our knowledge, we provide for the first time theoretical analysis of the dynamics and properties of replay buffer such as its Markovity and the explicit probability measure induces by the replay buffer.
4. We demonstrate our findings in a simulation of sim-to-real, with two simulations where one is a distorted version of the other and analyze it empirically.

2 Related Work

Sim-to-Real: Sim-to-Real is a long investigated topic in robotics where one aims to reduce the reality gap between the real system and its digital twin implementation. A general framework where we transfer results from one domain to another is *domain adaptation*. In vision, this approach have helped to gain state-of-the-art results [16, 44, 33, 10, 24, 43]. In our work, we focus on the physical aspects of the sim-to-real gap. Related to domain adaptation, is the approach of *domain randomization*, where the randomization is done in simulation in order to robustify and enhance

the detection and object recognition capability [46, 41, 20, 48]. Recently, [21] proposed a method where both simulation and reality are adapted to a common domain. Andrychowicz et al. [2] extensively randomize the task of reaching a cube pose where one-shot transfer is achieved but with large sample complexity. Randomization may also be applied to dynamics, e.g., [36], where robustness to inaccuracy in real world parameters is achieved.

Another approach in Sim-to-Real is how to change the simulation in the light of real samples. In [12] the agent learns mainly from simulation but its parameters are updated to match the behavior in reality by reducing the difference between simulation and reality roll-outs. Our method is a direct approach that incorporates phenomena that is difficult to simulate accurately. In Bayesian context, [40] provide a principled framework to reason about the uncertainty in simulation parameters. Kang et al. [23] investigated how real system and simulation data can be combined in training deep RL algorithms. They separate between the data types by using real data to learn about the dynamics of the system, and simulated data to learn a generalizing perception system. Our method mix real and simulation data by controlling the rate of streaming each data type into the learning agent.

Replay Buffer analysis: Large portion of RL algorithms use replay buffers [31, 34] but here we review only works that provide some analysis. Several works study the effect of replay buffer size on the agent performance [52, 32]. Our focus is the effect of controlling the rate of collecting samples and the rate of using them in the optimization process. Fedus et al. [15] investigated the effect of the ratio between these rates on the learning process through simulated experiments, while our focus is on the theoretical aspects. Other works studied the criteria for prioritizing transitions to enhance learning [42, 35, 51]. In case of multiple agents that share their policy, Horgan et al. [17] argue in favor of a shared replay buffer for all agents and a prioritizing mechanism. We, on the other hand, emphasize the advantage of separating replay buffers when collecting samples from different environments to enable a mixing management in the learning process.

Stochastic Approximation: Our proposed algorithm is based on the Stochastic Approximation method [28]. Konda and Tsitsiklis [26] proposed the actor-critic algorithm, and established the asymptotic convergence for the two time-scale actor-critic, with TD(λ) learning-based critic. Bhatnagar et al. [5] proved the convergence result for the original actor-critic and natural actor-critic methods. Di Castro and Meir [14] proposed a single time-scale actor-critic algorithm and proved its convergence. Recently, several finite sample analyses were applied by [49, 53, 13] and more but these works have not analyzed the RB asymptotic behavior while we do.

3 Setup

We model the problem using a Markov Decision Process (MDP; [39]), where \mathcal{S} and \mathcal{A} are the state space and action space, respectively. We let $P(s'|s, a)$ denote the probability of transitioning from state $s \in \mathcal{S}$ to state $s' \in \mathcal{S}$ when applying action $a \in \mathcal{A}$. The MDP measure $P(s'|s, a)$ and the policy measure $\pi_\theta(a|s)$ induce together a Markov Chain (MC) measure $P_\theta(s'|s)$ (P_θ is matrix form). We consider a probabilistic policy $\pi_\theta(a|s)$, parameterized by $\theta \in \Theta \subset \mathbb{R}^d$ which expresses the probability of the agent to choose an action a given that it is in state s . We let μ_θ denote the stationary distribution induced by the policy π_θ . The reward function is denoted by $r(s, a)$. Throughout the paper we assume the following.

Assumption 1. 1. The set Θ is compact. 2. The reward $|r(\cdot, \cdot)| \leq 1$ for all $s \in \mathcal{S}, a \in \mathcal{A}$.

Assumption 2. For any policy π_θ , the induced Markov chain of the MDP process $\{s_\tau\}_{\tau \geq 0}$ is irreducible and aperiodic.

The goal of the agent is to find a policy that maximizes the *average reward* that the agent receives during its interaction with the environment [39]. Under an ergodicity assumption, the average reward over time eventually converges to the expected reward under the stationary distribution [3]

$$\eta_\theta \triangleq \lim_{T \rightarrow \infty} \frac{\sum_{\tau=0}^T r(s_\tau, a_\tau)}{T} = \mathbb{E}_{s \sim \mu_\theta, a \sim \pi_\theta} [r(s, a)]. \quad (1)$$

The state-value function evaluates the overall expected accumulated rewards given a starting state s and a policy π_θ

$$V^{\pi_\theta}(s) \triangleq \mathbb{E} \left[\sum_{\tau=0}^{\infty} (r(s_\tau, a_\tau) - \eta_\theta) \middle| s_0 = s, \pi_\theta \right], \quad (2)$$

where the actions follow the policy $a_\tau \sim \pi_\theta(\cdot|s_\tau)$ and the next state follows the transition probability $s_{\tau+1} \sim P(\cdot|s_\tau, a_\tau)$. Denote \mathbf{v}^θ to be the vector value function defined in (2). Therefore, the vectorial Bellman Equation (BE) for a fixed policy $\pi_\theta(\cdot, \cdot)$ is $\mathbf{v}^\theta = r - \eta_\theta + P_\theta \mathbf{v}^\theta$, where r is a vector of rewards for each state [39]. We recall that the solution to the BE is unique up to an additive constant. In order to have a unique solution, we choose a state s^* to be of value 0, i.e., $V^{\pi_\theta}(s^*) = 0$ (due to Assumption 2, s^* can be any of $s \in S$).

In our specific setup, we consider a model where there are K MDPs, denoted by M_k , all share the same state space \mathcal{S} , action space \mathcal{A} , and reward function $r(s, a)$. The environment dynamics, though, are different, and are denoted by a transition function $P_k(\cdot|\cdot, \cdot)$. Together with a shared policy $\pi_\theta(\cdot|\cdot)$, each M_k is induced by a state transition measure $P_{\theta,k}(s'|s)$ and a stationary distribution $\mu_{\theta,k}$. Let $\eta_{\theta,k} = \mathbb{E}_{s \sim \mu_{\theta,k}, a \sim \pi_\theta} [r(s, a)]$ and define the average reward over K environments,

$$\bar{\eta}_\theta = \mathbb{E}_{k \sim \beta, s \sim \mu_{\theta,k}, a \sim \pi_\theta} [r(s, a)] = \sum_{k=1}^K \beta_k \eta_{\theta,k}. \quad (3)$$

The following assumption resembles Assumption 2 for K environments.

Assumption 3. *For any policy π_θ , the induced Markov chain of MDP M_k is irreducible and aperiodic for all $k = 1 \dots K$.*

We define ν_k to be the *throughput* of M_k and it is defined as the number of samples MDP M_k provides for a unit time. In sim-to-real context, this setup can practically handle several robots and several simulation instances. We assume for the sim-to-real scenario that $\nu_s > \nu_r$.

Since the samples from real arrive at a lower throughput than the sim, if we push the samples into two separate Replay Buffers (RB; [31, 34]) based on their sources, we can leverage the relatively scarce, but valuable samples that originated in the real system. This observation is the main motivation for our "Mixing Sim and Real" scheme, presented in the next section.

4 Mixing Sim and Real Algorithm

In order to reconcile the dynamics disparity, we propose our *Mixing Sim and Real Algorithm with Linear Actor Critic*, presented in Algorithm 1 and described in Figure 1. We consider K environments, modeled as MDPs, M_1, \dots, M_K , where the agent maintain a replay buffer $RB(k)$ for each MDP, respectively. For the sake of analysis simplicity, we replace $\{\nu_k\}$ with the following random variable. The agent chooses an environment to communicate with according to $I \sim \text{Categorical}(q_1, \dots, q_K)$ where $q \triangleq [q_1, \dots, q_K]$, $q_i \geq 0$, and $\sum_i q_i = 1$. The agent collects transitions $\{s_i, a_i, r_i, s'_i\}$ from the chosen environment and stores them in the corresponding $RB(i)$. In order to approximate the rates $\{\nu_k\}_{k=1}^K$ correctly, we choose $q_i = \nu_i / \sum_k \nu_k$ for the agent to interact according to the rates.

Algorithm 1 Mixing Sim and Real with Linear Actor Critic

- 1: Initialize Replay Buffers $RB(k)$ with size N and initialize $t_k = 0$ for $k = 1, \dots, K$.
 - 2: Initialize actor parameters θ_0 , critic parameters v_0 and average reward estimator η_0 .
 - 3: **for** $\tau = 0, \dots$ **do**
 - 4: Sample $i \sim q$, interact with M_i according to policy π_{θ_τ} and add the transition $\{s_{i,t_i}, a_{i,t_i}, r_{i,t_i}, s_{i,t_i+1}\}$ to $RB(i)$. Increment $t_i \leftarrow t_i + 1$.
 - 5: Sample $j \sim \beta$ and choose N_{batch} transitions from $RB(j)$ denoted as $\{\tilde{O}_{j,n}^z(\tau)\}_{z=1}^{N_{\text{batch}}}$.
 - 6: $\delta(\tilde{O}^z) = \tilde{r}^z - \eta_\tau + \phi(\tilde{s}'^z)^\top v_\tau - \phi(\tilde{s}^z)^\top v_\tau$
 - 7: Update average reward
 $\eta_{\tau+1} = \eta_\tau + \alpha_\tau^\eta \left(\frac{1}{N_{\text{batch}}} \sum_z \tilde{r}^z - \eta_\tau \right)$
 - 8: Update critic $v_{\tau+1} = v_\tau + \alpha_\tau^v \frac{1}{N_{\text{batch}}} \sum_z \delta(\tilde{O}^z) \phi(\tilde{s}^z)$
 - 9: Update actor $\theta_{\tau+1} = \Gamma \left(\theta_\tau - \alpha_\tau^\theta \frac{1}{N_{\text{batch}}} \sum_z \delta(\tilde{O}^z) \nabla_\theta \log \pi_\theta(\tilde{a}^z | \tilde{s}^z) \right)$
 - 10: **end for**
-

We train the agent in an off-policy manner. The agent selects $RB(j)$ for sampling the next batch for training according to $J \sim \text{Categorical}(\beta_1, \dots, \beta_K)$ where $\beta \triangleq [\beta_1, \dots, \beta_K]$, $\beta_j \geq 0$, and $\sum_j \beta_j =$

1. This distribution remains static, and hence the selections in time are i.i.d². In addition, the β distribution that selects which samples to train over should be different than the q distribution that controls the throughput each environments pushes samples to the RB. In that way, scarce samples from the real environment can get higher influence on the training.

Once a RB is selected, the sampled batch is used for optimizing the actor and the critic parameters. In this work, we propose a two time scale linear actor critic optimization scheme [26], which is an RB-based version of [5] Algorithm. We analyze its convergence properties in Section 5. We note, however, that other optimization schemes can be provided, such as DDPG [30], which we use in our experiments.

We define a tuple of indices (k, n) where k corresponds to $RB(k)$ and n corresponds to the n -th sample in this $RB(k)$. In addition, it corresponds to time $t(k, n)$ where this is the time when the agent interacted with the k -th MDP and the n -sample was added to $RB(k)$. Let $\tilde{\mathcal{O}}_{k,n}(\tau) \triangleq \{\tilde{s}_{k,n}, \tilde{a}_{k,n}, \tilde{r}_{k,n}, \tilde{s}'_{k,n}\}$ be a transition sampled at time τ from $RB(k)$. Whenever it is clear from the context, we simply use $\tilde{\mathcal{O}}$.

The temporal difference (TD) error $\delta(\tilde{\mathcal{O}})$ is a random quantity based on a single sampled transition from $RB(k)$,

$$\delta(\tilde{\mathcal{O}}) = r(\tilde{s}, \tilde{a}) - \eta + \phi(\tilde{s}')^\top v - \phi(\tilde{s})^\top v, \quad (4)$$

where $\hat{V}_v^{\pi_\theta}(s) = \phi(s)^\top v$ is a linear approximation for $V^{\pi_\theta}(s)$, $\phi(s) \in \mathbb{R}^d$ is a feature vector for state s and $v \in \mathbb{R}^d$ is a parameter vector. In Algorithm 1, average reward, critic and actor parameters are updated based on the TD error (see lines 7 - 9). Note that for the actor updates, we use a projection $\Gamma(\cdot)$ that projects any $\theta \in \mathbb{R}^d$ to a compact set Θ whenever $\theta \notin \Theta$.

In order to gain understanding of our proposed setup, in the next section we characterize the behaviour of the iterations in Algorithm 1.

5 Convergence Analysis for Mixing Sim and Real with Linear Approximation

The standard tool in the literature for analyzing iterations of processes such as two time scale Actor-Critic in the context of RL is *SA; Stochastic Approximation* [27, 8, 4]. This analysis technique includes two parts: proving the existence of a fixed point, and bounding the rate of convergence to this fixed point. By far, the most popular methods for proving convergence is the *Ordinary Differential Equation (ODE) method*. Usually, the iteration should demonstrate either some monotonicity property, or a contraction feature in order for the iteration to converge.

Although in practice such algorithms (after some tuning) usually converge to an objective value, it is not always guaranteed. To achieve that in a stochastic approximation setup, the main known result shows that the iteration can be decomposed into a deterministic function, which depends only on the problem parameters, and a martingale difference noise, which is bounded in some way.

In this section we show that the iterations of Algorithm 1 converge to a stable point of a corresponding ODE. We begin with showing that the process of sampling transitions from RBs is a Markov process. Afterward, we show that if the original Markov chain is irreducible and aperiodic, then also the RBs Markov process is irreducible and aperiodic. This property is required for proving the convergence of the iterations in Algorithm 1 using SA tools. We conclude this section with showing that if in some sense sim is close to real, then the properties of the mixed process is close to the properties of both sim and real.

5.1 Asymptotic Convergence of Algorithm 1

Let $RB(k)$ be a replay buffer storing the last N transitions from MDP k . Let $RB_\tau(k)$ be the state of $RB(k)$ at time τ , i.e., $RB_\tau(k) \triangleq \{\mathcal{O}_{k,1}, \dots, \mathcal{O}_{k,N}\}$, where $\mathcal{O}_{k,n} = \{s_{k,n}, a_{k,n}, r_{k,n}, s'_{k,n}\}$ is a transition tuple pushed at some time $t(k, n) < \tau$. We denote the collection of all $RB_\tau(k)$ as

²We note that one could remove this restriction and think of other schemes in which the replay buffer selection distribution changes over time based on some prescribed optimization goal, cost, etc.

$\bigcup_{k=1}^K RB_\tau(k)$. We define I_τ and J_τ be i.i.d random processes based on I and J , respectively. We define Y_τ to be the process induced by Algorithm 1, i.e.,

$$Y_\tau = \left[\bigcup_{k=1}^K RB_\tau(k), I_\tau, J_\tau \right]. \quad (5)$$

The next lemma states the Y_τ is Markovian. The proof is deferred to the Supplementary material A.1.

Lemma 1 (Y_τ induced by Algorithm 1 is Markovian). *1. The random process Y_τ is a Markovian. 2. Under Assumption 3, there exists some $\tau' > 0$ such that Y_τ is irreducible and aperiodic for $\tau \geq \tau'$.*

Next, we present several assumptions that are necessary for proving the convergence of Algorithm 1. The first assumption is a standard requirement for policy gradient methods.

Assumption 4. *For any state–action pair (s, a) , $\pi_\theta(a|s)$ is continuously differentiable in the parameter θ .*

Proving convergence for a general function approximation is hard. In our case we demonstrate the convergence for a linear function approximation (LFA; [4]). In matrix form, it can be expressed as $V = \Phi v$ where $\Phi \in \mathbb{R}^{|S| \times d}$. The following assumption is needed for the uniqueness of the convergence point of the critic.

Assumption 5. *1. The matrix Φ has full rank. 2. The functions $\phi(s)$ are Lipschitz in s and bounded. 3. For every $v \in \mathbb{R}^d$, $\Phi v \neq e$ where e is a vector of ones.*

In order to get a *with probability 1* using the SA convergence, the following standard assumption is needed. Note that in the actor-critic setup we need two time-scales convergence, thus, in this assumption the critic is a ‘faster’ recursion than the actor.

Assumption 6. *The step-sizes $\{\alpha_\tau^\eta\}$, $\{\alpha_\tau^v\}$, $\{\alpha_\tau^\theta\}$, $\tau \geq 0$ satisfy $\sum_\tau \alpha_\tau^\eta = \sum_\tau \alpha_\tau^v = \sum_\tau \alpha_\tau^\theta = \infty$, $\sum_\tau (\alpha_\tau^\eta)^2 < \infty$, $\sum_\tau (\alpha_\tau^v)^2 < \infty$, $\sum_\tau (\alpha_\tau^\theta)^2 < \infty$ and $\alpha_\tau^\theta = o(\alpha_\tau^v)$.*

We define the induced MC for the time $t(k, n)$ with a corresponding parameter $\theta_{t(k, n)}$. For this parameter, we denote with $P_{t(k, n)}$ the transition matrix at that time and the corresponding state distribution vector $\rho_{t(k, n)}$ (both induced by the policy $\pi_{\theta_{t(k, n)}}$). Finally, we define the following diagonal matrix $S_{t(k, n)} \triangleq \text{diag}(\rho_{t(k, n)})$ and the reward vector $r_{t(k, n)}$ with elements $r_{t(k, n)}(s) = \sum_a \pi_{\theta_{t(k, n)}}(a|s)r(s, a)$. Based on these definitions we define

$$A_\tau \triangleq \sum_{k=1}^K \sum_{n=1}^N \frac{\beta_k}{N} S_{t(k, n)} (P_{t(k, n)} - I), \quad b_\tau \triangleq \sum_{k=1}^K \sum_{n=1}^N \frac{\beta_k}{N} S_{t(k, n)} (r_{t(k, n)} - \eta_{\theta, k} e). \quad (6)$$

where I is the identity matrix and e is a vector of ones. The intuition behind A_τ and b_τ is the following. For an online TD(0)-learning under a stationary policy we have a fixed point at the solution to the equation $\Phi^\top D(P - I)\Phi v + \Phi^\top D(r - \eta) = 0$ ([4]; Lemma 6.5). In our case, since we have K RBs where each one with N samples entered at different times, we have a superposition of all these samples. When $\tau \rightarrow \infty$, $\rho_{t(k, n)} \rightarrow \mu_{\theta, k}$ for all index n . We let $S_{\theta, k} \triangleq \text{diag}(\mu_{\theta, k})$ and define

$$A_\theta \triangleq \sum_{k=1}^K \beta_k S_{\theta, k} (P_{\theta, k} - I), \quad b_\theta \triangleq \sum_{k=1}^K \beta_k S_{\theta, k} (r_{\theta, k} - \eta_{\theta, k} e). \quad (7)$$

For proving the convergence of the critic, we assume the policy is fixed. Thus, for each RB the induced MC is one for all the samples in this RB, so the sum over N disappear for A_θ and b_θ . Now we are ready to prove the following theorems, regarding Algorithm 1. We note that Theorems 2 and 3 state the critic and actor convergence.

Theorem 2. *(Convergence of the Critic to a fixed point)*

Under Assumptions 1-6, for any given π and $\{\eta_\tau\}$, $\{v_\tau\}$ as in the updates in Algorithm 1, we have $\eta_\tau \rightarrow \bar{\eta}$ and $v_\tau \rightarrow v^\pi$ with probability 1, where v^π is obtained as a unique solution to $\Phi^\top A_\theta \Phi v + \Phi^\top b_\theta = 0$.

The proof for Theorem 2 follows the proof for Lemma 5 in [7], see more details in the supplementary material A.2. For establishing the convergence of the actor updates, we define additional terms. Let \mathcal{Z} denote the set of asymptotically stable equilibria of the ODE $\dot{\theta} = \hat{\Gamma}(-\nabla_{\theta}\bar{\eta}_{\theta})$ and let \mathcal{Z}^{ϵ} be the ϵ -neighborhood of \mathcal{Z} . Let $\bar{V}_k^{\pi_{\theta}}(\tilde{s}) = \sum_{\tilde{a}} \pi_{\theta}(\tilde{a}|\tilde{s}) (r(\tilde{s}, \tilde{a}) - \eta_{\theta,k} + \sum_{\tilde{s}'} P_k(\tilde{s}'|\tilde{s}, \tilde{a})\phi(\tilde{s}')^{\top} v^{\pi_{\theta}})$, and define

$$\xi^{\pi_{\theta}} = \sum_{k=1}^K \beta_k \sum_{\tilde{s}} \mu_{\theta,k}(\tilde{s}) \left(\phi(\tilde{s})^{\top} \nabla_{\theta} v^{\pi_{\theta}} - \nabla_{\theta} \bar{V}_k^{\pi_{\theta}}(\tilde{s}) \right).$$

Theorem 3. (*Convergence of the actor*)

Under Assumptions 1-6, given $\epsilon > 0$, $\exists \delta > 0$ such that for θ_{τ} , $\tau \geq 0$ obtained using Algorithm 1, if $\sup_{\theta_{\tau}} \|\xi^{\pi_{\theta_{\tau}}}\| < \delta$, then $\theta_{\tau} \rightarrow \mathcal{Z}^{\epsilon}$ as $\tau \rightarrow \infty$ with probability one.

The proof for Theorem 3 follows the proof for Theorem 2 in [7] and is given in the supplementary material A.3.

5.2 Sim2Real Asymptotic Convergence Properties

In this section we analyze the convergence properties of the Mixing Sim and Real algorithm we use. The main idea is that if sim and real are close in their dynamics through the MDP transition matrix many properties of their MDPs under the same policy are close as well. Moreover, we show that under the assumption of sim close to real, any process derived from both processes is close to both sim and real.

Assumption 7. (*Closeness of sim and real*). For all θ , $s, s' \in S$, $a \in A$, we have $|P_s(s'|s, a) - P_r(s'|s, a)| \leq \epsilon_{s2r}$.

The following theorem states that if Assumption 7 holds then the convergence points of sim, real, and the mixed process (as defined in Algorithm 1) convergences to close points.

Theorem 4. Consider a policy $\pi_{\theta}(a|s)$ and Assumptions 1, 2, and 7. Then, for each $s, s' \in S$, $a \in A$, and $\forall \theta \in \Theta$ we have:

1. The induced MC of sim and real, MC_s and MC_r , satisfy $|P_s^{\theta}(s'|s) - P_r^{\theta}(s'|s)| \leq B_P \triangleq |A|\epsilon_{s2r}$.
2. Let $\tilde{P}_s^{\theta} \in \mathbb{R}^{(|S|-1) \times (|S|-1)}$ where its elements are identical to the first $(|S|-1) \times (|S|-1)$ elements of P_s^{θ} . The corresponding stationary distributions satisfy $|\mu_s^{\theta}(s) - \mu_r^{\theta}(s)| \leq B_{\mu} \triangleq B_P |S|^3 \min_{\theta \in \Theta} \sqrt{SR_m^2}$, where R_m is the largest eigenvalue of the matrix \tilde{P}_s^{θ} .
3. The convergence points for the average reward and value functions under the policy for sim and real satisfy $\|\eta_s^{\theta} - \eta_r^{\theta}\| \leq B_{\eta} \triangleq B_{\mu}|S|$ and $\|\mathbf{v}_s^{\theta} - \mathbf{v}_r^{\theta}\| \leq B_{\mu}$.

The proof for Theorem 4 is in the supplementary material B. Based on this Theorem, it follows immediately that any convex combination of "close" enough sim and real share the same properties as both sim and real. We defer to supplementary material the precise statement.

6 Experimental Evaluation

In this section we evaluate the performance of our proposed algorithm on two Fetch Push environments [38], one acts as the real environment and the other is the simulation environment³. Although our theoretical results are on the proposed mixing scheme with linear function approximation, in this section we focus on non-linear methodologies, i.e., using neural networks. We set $K = 2$ meaning there is only one real and one simulation environments. We denote by q_r the probability of collecting samples from the real environment and by β_r the probability of choosing samples from the real environment for the optimization process. We are interested in demonstrating the effect of different q_r and β_r values on the learning process. We investigate different mixing strategies for combining real and sim samples.

1. "Mixed": real and sim episodes are collected according to Algorithm 1.
2. "Real only": The agent collects and optimize only real samples (i.e., $q_r = 1$ and $\beta_r = 1$).
3. "Sim only": The agent collects and optimize only sim samples (i.e., $q_r = 0$ and $\beta_r = 0$).

³Code for the experiments can be available at: <https://github.com/sdicastro/SimAndRealBetterTogether>.

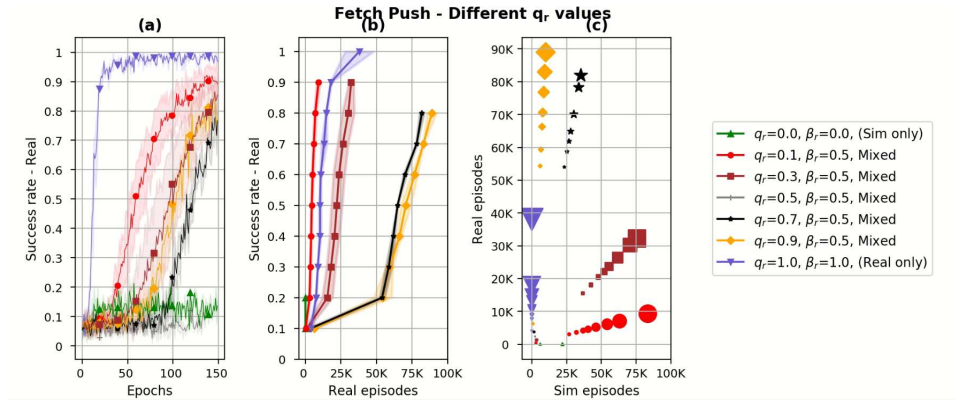


Figure 2: "Real only", "Sim only", and "Mixed" strategies with fixed β_r and different q_r values. **(a)** Success rate in the real environment vs. number of epochs. Each epoch corresponds to 100 episodes, mixed with real and sim episodes. The success rate is computed every epoch over 10 test episodes. **(b)** Success rate in the real environment vs. number of real episodes **(c)** Number of real episodes vs. number of sim episodes. The size of the markers corresponds to the increasing success rate. For all graphs, we repeated each experiment with 10 different random seeds and present the mean and standard deviation values.

4. "Sim first": At the beginning the agent collects and optimize only sim samples. When the success rate in the sim reaches 0.7, we switch to sampling and optimizing only using real.
5. "Sim-dependent": At the beginning the agent collects and optimize only sim samples. When the success rate in the sim environment reaches 0.7, we switch to the "Mixed" strategy.

In the Fetch Push task, a robot arm needs to push an object on a table to a certain goal point. The state is represented by the gripper, object and target position and pose, as well as their velocities and angular velocities⁴. The action specifies the desired gripper position at the next time-step. The agent gets a reward of -1, if the desired goal was not yet achieved and 0 if it was achieved within some tolerance. To solve the task we used our mixing sim and real algorithm and replaced the linear actor-critic optimization scheme (lines 6-9 in Algorithm 1) with DDPG [30] together with Hindsight Experience Replay (HER; [1]) optimization scheme. We created the real and sim environments using the Mujoco simulator [47]. The difference between the environments is the friction between the object and the table. We preceded the following experiments with an experiment to depict a region of friction parameters where training the task using only sim samples and using the trained policy in the real environment does not solve the task (see supplementary material Section C.3).

We emphasize that we evaluate the performance in each experiment according to the success rate in the *real environment*, as this is the environment of final interest. In addition, we seek for mixing strategies that achieve the *lowest* number of *real* samples since usually they are costly and harder to get than sim samples.

Different q_r values: We fix optimization parameter $\beta_r = 0.5$ and test different collection parameter $q_r = 0, 0.1, 0.3, 0.5, 0.7, 0.9, 1$. Results are presented in Figure 2. We notice that when the agent is trained using "Sim only" strategy ($q_r = 0$), it fails to solve the task in real (Figure 2a). Next, when the agent is trained using "Real only" strategy ($q_r = 1$), the task is solved. However, for achieving 0.9 success rate, "Real only" requires approximately 20K real environment episodes and to increase it to success rate of 1, it requires approximately 40K real episodes (Figures 2b and 2c). Observing the q_r values in-between, we see that $q_r = 0.1$ achieves the best performance – it uses fewer ($\approx 10K$) real episodes to achieve high success rates compared to the "Real only" strategy. Notice that as q_r increases the performance deteriorates. This phenomenon can be explained due to the mixed samples distribution. When q_r is low, most of the data distribution is based on sim, and real samples do not change it much, but only "fine tune" the learning. When q_r increases, the data distribution is composed of two different environments which may confuse the agent.

⁴The final dimension is 28 after removing non-informative dimensions.

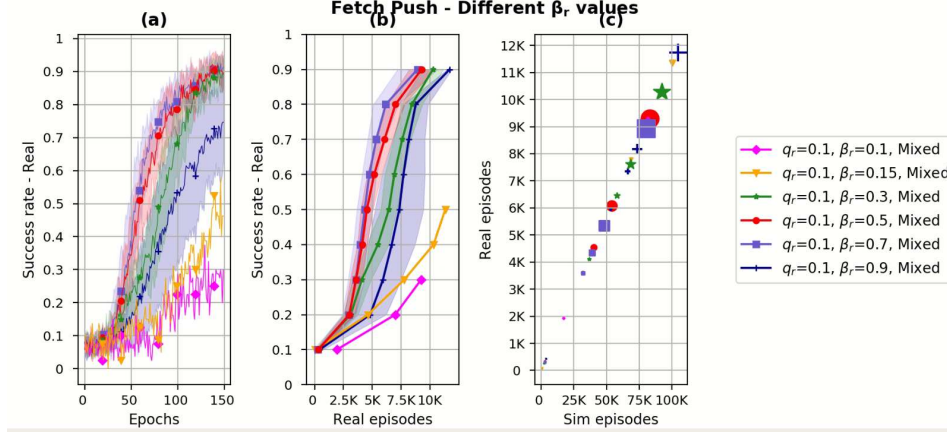


Figure 3: The "Mixed" strategy with fixed q_r and different β_r values. (a), (b) and (c) descriptions are the same as in Figure 2. In (c), the size of the markers corresponds to the increasing success rate: 0.1, 0.3, 0.5, 0.7, 0.9.

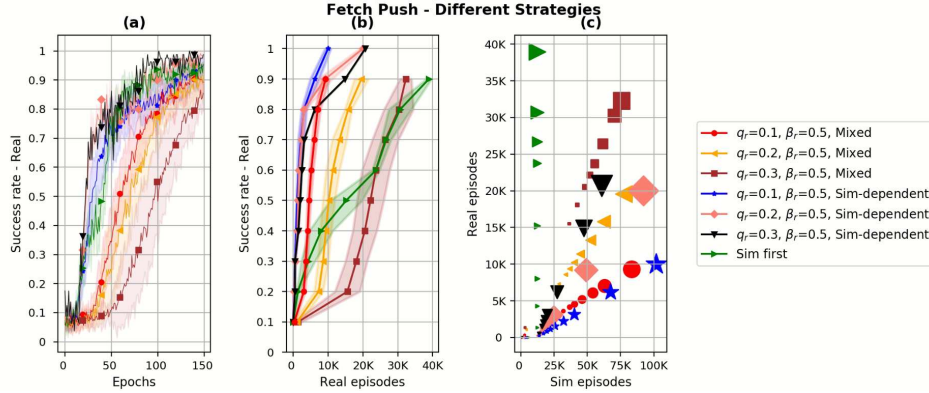


Figure 4: Comparing strategies: "Mixed", "Sim-dependent" and "Sim first". (a), (b) and (c) descriptions are the same as in Figure 2. It can be clearly seen in (c) that "Sim first" requires the most number of real episodes to achieve a high success rate. In addition, (b) and (c) demonstrate that for the same (q_r, β_r) tuple, for example $(q_r = 0.2, \beta_r = 0.5)$, "Sim-dependent" strategy achieves higher success rates with less number of real episodes, compared to the "Mixing" strategy.

Different β_r values: In this experiment, we fix $q_r = 0.1$ and test for $\beta_r = 0.1, 0.15, 0.3, \dots, 0.9$. Results are presented in Figure 3. When β_r is low and equals q_r , the agent fails to solve the task (Figure 3a). But when β_r is higher than q_r , the performance improves where no significant differences are observed for $\beta_r = 0.3, 0.5, 0.7$. For $\beta_r = 0.7$, the algorithm achieves the best performance: high success rate of 0.9 while using fewer real episodes and fewer sim episodes compared to other β_r values (Figures 3b and 3c). Interestingly, when β_r is too high (with respect to q_r , i.e., $\beta_r = 0.9$) the performance deteriorates, suggesting that choosing $\beta_r > q_r$ is preferable.

Different Mixing Strategies: We tested different mixing strategies. "Mixed", "Sim first" and "Sim-dependent" as described above. Results are presented in Figure 4. Using the "Sim-dependent" strategy reduced the required real and sim episodes to achieve 0.9 success rate comparing to the "Mixed" strategy with the same q_r and β_r values (Figure 4c). When using "Sim first" strategy, we observe that although in the beginning of the learning it uses only sim samples, once it switches to use only real samples, the agent requires many more real episodes to achieve success rate of 0.9 (compared to the "Mixed" and "Sim-dependent" strategies; Figures 4b and 4c). Although the most common approach is to train a policy in simulation and then use it as an initial starting point for the real system, we see that applying the mixing strategy after transferring the policy to real can reduce further the required real episodes while maintaining high success rate.

7 Conclusions and Future Work

In this work we analyzed a mixing strategy between simulation and real system samples. By separating the rate of collecting samples from each environment and the rate of choosing samples for the optimization process, we were able to achieve a significant reduction in the amount of real environment samples, comparing to the common strategy of using the same rate for both collection and optimization phases. This reduction is of special interest since usually the real samples are costly and harder to achieve. We believe this work can lead to a new line of research. First, finite sample analysis for our proposed algorithm can reveal its exact sample complexity. Comparing it to the sample complexity of learning only on real environment can emphasize the advantage of using the mixing strategy. Second, other replay buffer prioritization schemes can now be theoretically analyzed using the dynamics and properties of replay buffers we have developed. Third, our approach is limited to the online case, where new samples are collected during training. Adapting our approach to the offline case can discover new venues in the offline RL research. Fourth, learning the real samples collection rate and adapting it during training can further improve our approach.

References

- [1] Marcin Andrychowicz, Filip Wolski, Alex Ray, Jonas Schneider, Rachel Fong, Peter Welinder, Bob McGrew, Josh Tobin, OpenAI Pieter Abbeel, and Wojciech Zaremba. Hindsight experience replay. In *Advances in neural information processing systems*, pages 5048–5058, 2017.
- [2] OpenAI: Marcin Andrychowicz, Bowen Baker, Maciek Chociej, Rafal Jozefowicz, Bob McGrew, Jakub Pachocki, Arthur Petron, Matthias Plappert, Glenn Powell, Alex Ray, et al. Learning dexterous in-hand manipulation. *The International Journal of Robotics Research*, 39(1):3–20, 2020.
- [3] D. Bertsekas. *Dynamic programming and optimal control*. Athena scientific Belmont, MA, 2005.
- [4] Dimitri P Bertsekas and John N Tsitsiklis. *Neuro-dynamic programming*. Athena Scientific, 1996.
- [5] Shalabh Bhatnagar, Mohammad Ghavamzadeh, Mark Lee, and Richard S Sutton. Incremental natural actor-critic algorithms. In *Advances in neural information processing systems*, pages 105–112, 2008.
- [6] Shalabh Bhatnagar and Shishir Kumar. A simultaneous perturbation stochastic approximation-based actor-critic algorithm for markov decision processes. *IEEE Transactions on Automatic Control*, 49(4):592–598, 2004.
- [7] Shalabh Bhatnagar, Richard S Sutton, Mohammad Ghavamzadeh, and Mark Lee. Natural actor-critic algorithms. *Automatica*, 45(11):2471–2482, 2009.
- [8] Vivek S Borkar. *Stochastic approximation: a dynamical systems viewpoint*, volume 48. Springer, 2009.
- [9] Vivek S Borkar and Sean P Meyn. The ode method for convergence of stochastic approximation and reinforcement learning. *SIAM Journal on Control and Optimization*, 38(2):447–469, 2000.
- [10] Konstantinos Bousmalis, George Trigeorgis, Nathan Silberman, Dilip Krishnan, and Dumitru Erhan. Domain separation networks. In *Advances in neural information processing systems*, pages 343–351, 2016.
- [11] James Bucklew. *Introduction to rare event simulation*. Springer Science & Business Media, 2013.
- [12] Yevgen Chebotar, Ankur Handa, Viktor Makoviychuk, Miles Macklin, Jan Issac, Nathan Ratliff, and Dieter Fox. Closing the sim-to-real loop: Adapting simulation randomization with real world experience. In *2019 International Conference on Robotics and Automation (ICRA)*, pages 8973–8979. IEEE, 2019.
- [13] Gal Dalal, Balázs Szörényi, Guga Thoppe, and Shie Mannor. Finite sample analyses for td (0) with function approximation. In *Proceedings of the AAAI Conference on Artificial Intelligence*, 2018.

- [14] Dotan Di Castro and Ron Meir. A convergent online single time scale actor critic algorithm. *The Journal of Machine Learning Research*, 11:367–410, 2010.
- [15] William Fedus, Prajit Ramachandran, Rishabh Agarwal, Yoshua Bengio, Hugo Larochelle, Mark Rowland, and Will Dabney. Revisiting fundamentals of experience replay. In *International Conference on Machine Learning*, pages 3061–3071. PMLR, 2020.
- [16] Yaroslav Ganin, Evgeniya Ustinova, Hana Ajakan, Pascal Germain, Hugo Larochelle, François Laviolette, Mario Marchand, and Victor Lempitsky. Domain-adversarial training of neural networks. In *Domain Adaptation in Computer Vision Applications*, pages 189–209. Springer, 2017.
- [17] Dan Horgan, John Quan, David Budden, Gabriel Barth-Maron, Matteo Hessel, Hado Van Hasselt, and David Silver. Distributed prioritized experience replay. *arXiv preprint arXiv:1803.00933*, 2018.
- [18] Roger A Horn and Charles R Johnson. *Matrix analysis*. Cambridge university press, 2012.
- [19] Nick Jakobi, Phil Husbands, and Inman Harvey. Noise and the reality gap: The use of simulation in evolutionary robotics. In *European Conference on Artificial Life*, pages 704–720. Springer, 1995.
- [20] Stephen James, Andrew J Davison, and Edward Johns. Transferring end-to-end visuomotor control from simulation to real world for a multi-stage task. *arXiv preprint arXiv:1707.02267*, 2017.
- [21] Stephen James, Paul Wohlhart, Mrinal Kalakrishnan, Dmitry Kalashnikov, Alex Irpan, Julian Ibarz, Sergey Levine, Raia Hadsell, and Konstantinos Bousmalis. Sim-to-real via sim-to-sim: Data-efficient robotic grasping via randomized-to-canonical adaptation networks. In *Proceedings of the IEEE Conference on Computer Vision and Pattern Recognition*, pages 12627–12637, 2019.
- [22] Dmitry Kalashnikov, Alex Irpan, Peter Pastor, Julian Ibarz, Alexander Herzog, Eric Jang, Deirdre Quillen, Ethan Holly, Mrinal Kalakrishnan, Vincent Vanhoucke, et al. Qt-opt: Scalable deep reinforcement learning for vision-based robotic manipulation. *arXiv preprint arXiv:1806.10293*, 2018.
- [23] Katie Kang, Suneel Belkhale, Gregory Kahn, Pieter Abbeel, and Sergey Levine. Generalization through simulation: Integrating simulated and real data into deep reinforcement learning for vision-based autonomous flight. In *2019 International Conference on Robotics and Automation (ICRA)*, pages 6008–6014. IEEE, 2019.
- [24] Taeksoo Kim, Moon-su Cha, Hyunsoo Kim, Jung Kwon Lee, and Jiwon Kim. Learning to discover cross-domain relations with generative adversarial networks. In *Proceedings of the 34th International Conference on Machine Learning-Volume 70*, pages 1857–1865. JMLR. org, 2017.
- [25] Diederik P Kingma and Jimmy Ba. Adam: A method for stochastic optimization. *arXiv preprint arXiv:1412.6980*, 2014.
- [26] Vijay R Konda and John N Tsitsiklis. Actor-critic algorithms. In *Advances in neural information processing systems*, pages 1008–1014. Citeseer, 2000.
- [27] Harold Kushner and G George Yin. *Stochastic approximation and recursive algorithms and applications*, volume 35. Springer Science & Business Media, 2003.
- [28] Harold Joseph Kushner and Dean S Clark. *Stochastic approximation methods for constrained and unconstrained systems*, volume 26. Springer Science & Business Media, 2012.
- [29] Sergey Levine, Peter Pastor, Alex Krizhevsky, Julian Ibarz, and Deirdre Quillen. Learning hand-eye coordination for robotic grasping with deep learning and large-scale data collection. *The International Journal of Robotics Research*, 37(4-5):421–436, 2018.
- [30] Timothy P Lillicrap, Jonathan J Hunt, Alexander Pritzel, Nicolas Heess, Tom Erez, Yuval Tassa, David Silver, and Daan Wierstra. Continuous control with deep reinforcement learning. *arXiv preprint arXiv:1509.02971*, 2015.
- [31] Long-Ji Lin. Reinforcement learning for robots using neural networks. Technical report, Carnegie-Mellon Univ Pittsburgh PA School of Computer Science, 1993.

- [32] Ruishan Liu and James Zou. The effects of memory replay in reinforcement learning. In *2018 56th Annual Allerton Conference on Communication, Control, and Computing (Allerton)*, pages 478–485. IEEE, 2018.
- [33] Mingsheng Long, Yue Cao, Jianmin Wang, and Michael I Jordan. Learning transferable features with deep adaptation networks. In *Proceedings of the 32nd International Conference on International Conference on Machine Learning-Volume 37*, pages 97–105. JMLR. org, 2015.
- [34] Volodymyr Mnih, Koray Kavukcuoglu, David Silver, Alex Graves, Ioannis Antonoglou, Daan Wierstra, and Martin Riedmiller. Playing atari with deep reinforcement learning. *arXiv preprint arXiv:1312.5602*, 2013.
- [35] Yangchen Pan, Muhammad Zaheer, Adam White, Andrew Patterson, and Martha White. Organizing experience: a deeper look at replay mechanisms for sample-based planning in continuous state domains. *arXiv preprint arXiv:1806.04624*, 2018.
- [36] Xue Bin Peng, Marcin Andrychowicz, Wojciech Zaremba, and Pieter Abbeel. Sim-to-real transfer of robotic control with dynamics randomization. In *2018 IEEE international conference on robotics and automation (ICRA)*, pages 1–8. IEEE, 2018.
- [37] Lerrel Pinto and Abhinav Gupta. Supersizing self-supervision: Learning to grasp from 50k tries and 700 robot hours. In *2016 IEEE international conference on robotics and automation (ICRA)*, pages 3406–3413. IEEE, 2016.
- [38] Matthias Plappert, Marcin Andrychowicz, Alex Ray, Bob McGrew, Bowen Baker, Glenn Powell, Jonas Schneider, Josh Tobin, Maciek Chociej, Peter Welinder, et al. Multi-goal reinforcement learning: Challenging robotics environments and request for research. *arXiv preprint arXiv:1802.09464*, 2018.
- [39] Martin L Puterman. *Markov Decision Processes*. Wiley and Sons, 1994.
- [40] Fabio Ramos, Rafael Carvalhaes Possas, and Dieter Fox. Bayessim: adaptive domain randomization via probabilistic inference for robotics simulators. *arXiv preprint arXiv:1906.01728*, 2019.
- [41] Fereshteh Sadeghi and Sergey Levine. Cad2rl: Real single-image flight without a single real image. *arXiv preprint arXiv:1611.04201*, 2016.
- [42] Tom Schaul, John Quan, Ioannis Antonoglou, and David Silver. Prioritized experience replay. *arXiv preprint arXiv:1511.05952*, 2015.
- [43] Ashish Shrivastava, Tomas Pfister, Oncel Tuzel, Joshua Susskind, Wenda Wang, and Russell Webb. Learning from simulated and unsupervised images through adversarial training. In *Proceedings of the IEEE conference on computer vision and pattern recognition*, pages 2107–2116, 2017.
- [44] Rui Shu, Hung H Bui, Hirokazu Narui, and Stefano Ermon. A dirt-t approach to unsupervised domain adaptation. *arXiv preprint arXiv:1802.08735*, 2018.
- [45] R. S. Sutton and A. G. Barto. *Reinforcement learning: An introduction*. MIT press, 2018.
- [46] Josh Tobin, Rachel Fong, Alex Ray, Jonas Schneider, Wojciech Zaremba, and Pieter Abbeel. Domain randomization for transferring deep neural networks from simulation to the real world. In *2017 IEEE/RSJ International Conference on Intelligent Robots and Systems (IROS)*, pages 23–30. IEEE, 2017.
- [47] Emanuel Todorov, Tom Erez, and Yuval Tassa. Mujoco: A physics engine for model-based control. In *2012 IEEE/RSJ International Conference on Intelligent Robots and Systems*, pages 5026–5033. IEEE, 2012.
- [48] Quan Vuong, Sharad Vikram, Hao Su, Sicun Gao, and Henrik I Christensen. How to pick the domain randomization parameters for sim-to-real transfer of reinforcement learning policies? *arXiv preprint arXiv:1903.11774*, 2019.
- [49] Yue Wu, Weitong Zhang, Pan Xu, and Quanquan Gu. A finite time analysis of two time-scale actor critic methods. *arXiv preprint arXiv:2005.01350*, 2020.
- [50] Ali Yahya, Adrian Li, Mrinal Kalakrishnan, Yevgen Chebotar, and Sergey Levine. Collective robot reinforcement learning with distributed asynchronous guided policy search. In *2017 IEEE/RSJ International Conference on Intelligent Robots and Systems (IROS)*, pages 79–86. IEEE, 2017.

- [51] Daochen Zha, Kwei-Herng Lai, Kaixiong Zhou, and Xia Hu. Experience replay optimization. *arXiv preprint arXiv:1906.08387*, 2019.
- [52] Shangdong Zhang and Richard S Sutton. A deeper look at experience replay. *arXiv preprint arXiv:1712.01275*, 2017.
- [53] Shaofeng Zou, Tengyu Xu, and Yingbin Liang. Finite-sample analysis for sarsa with linear function approximation. *arXiv preprint arXiv:1902.02234*, 2019.

A Proof of Main Lemmas and Theorems of Section 5.1

A.1 Proof of Lemma 1

Proof. **1.** Proving Markovity requires that

$$P(Y_{\tau+1}|Y_\tau, Y_{\tau-1}, \dots, Y_0) = P(Y_{\tau+1}|Y_\tau). \quad (8)$$

Let us denote $\mathcal{O}_{n_1}^{n_2} \triangleq \{\mathcal{O}_{n_1}, \dots, \mathcal{O}_{n_2}\}$, $I_{n_1}^{n_2} \triangleq \{I_{n_1}, \dots, I_{n_2}\}$ and $J_{n_1}^{n_2} \triangleq \{J_{n_1}, \dots, J_{n_2}\}$. Recall that $\mathcal{O}_\tau = \{s_\tau, a_\tau, r_\tau, s_{\tau+1}\}$ and that the time index of entering a transition into RB(k) is $t(k, n) \in \{0, \dots, \tau - 1\}$ for all $k \in \{1, \dots, K\}$ and for all $n \in \{1, \dots\}$. Index n relates the position in RB(k) in which the transition is placed at time τ . In addition, recall that $\mathcal{O}_{k,n} = \{s_{k,n}, a_{k,n}, r_{k,n}, s'_{k,n}\}$ where $s'_{k,n} \sim P_k(\cdot|s_{k,n})$. Let $RB_\tau(k)$ be RB(k) of MDP M_k at time τ , denoted as $RB_\tau(k) \triangleq \{\mathcal{O}_{k,1}, \dots, \mathcal{O}_{k,N}\}_\tau \triangleq \mathcal{O}_{k,1}^{k,N}(\tau)$. We denote the collection of all $RB_\tau(k)$ as $\bigcup_{k=1}^K RB_\tau(k) \triangleq \bigcup_{k=1}^K \mathcal{O}_{k,1}^{k,N}(\tau)$.

Remark 1. Note that each time step that a transition enters some $RB(\cdot)$ is unique. That is, for a fixed τ , $t(k, n) \neq t(k', n)$ for all n and for $k \neq k'$. Moreover, $t(k, n) < t(k, n+1)$ for all k and all n . In addition, note that when a new transition is pushed into the RB, the oldest transition in the RB is thrown away, and all the transitions in the RB, move one index forward, that is $\mathcal{O}_{k,n+1}(\tau+1) = \mathcal{O}_{k,n}(\tau)$ for $n = 1, \dots, N-1$ and $\mathcal{O}_{k,1}(\tau+1) = \mathcal{O}_\tau$.

Computing the l.h.s. of (8) yields

$$\begin{aligned} P(Y_{\tau+1}|Y_\tau, Y_{\tau-1}, \dots, Y_0) &\stackrel{1}{=} P\left(\bigcup_{k=1}^K RB_{\tau+1}(k), I_{\tau+1}, J_{\tau+1} \middle| \bigcup_{k=1}^K RB_\tau(k), I_\tau, J_\tau, \dots, \bigcup_{k=1}^K RB_0(k), I_0, J_0\right) \\ &\stackrel{2}{=} P\left(\bigcup_{k=1}^K \mathcal{O}_{k,1}^{k,N}(\tau+1), I_{\tau+1}, J_{\tau+1} \middle| \bigcup_{k=1}^K \mathcal{O}_{k,1}^{k,N}(\tau), I_\tau, J_\tau, \dots, \bigcup_{k=1}^K \mathcal{O}_{k,1}^{k,N}(0), I_0, J_0\right) \\ &\stackrel{3}{=} P\left(\bigcup_{k=1}^K \mathcal{O}_{k,1}^{k,N}(\tau+1), I_{\tau+1}, J_{\tau+1} \middle| I_0^\tau, J_0^\tau, \bigcup_{k=1}^K \mathcal{O}_{k,1}^{k,N}(\tau), \dots, \bigcup_{k=1}^K \mathcal{O}_{k,1}^{k,N}(0)\right) \\ &\stackrel{4}{=} P\left(\bigcup_{k=1}^K \mathcal{O}_{k,1}^{k,N}(\tau+1) \middle| I_0^{\tau+1}, J_0^{\tau+1}, \bigcup_{k=1}^K \mathcal{O}_{k,1}^{k,N}(\tau), \dots, \bigcup_{k=1}^K \mathcal{O}_{k,1}^{k,N}(0)\right) \\ &\quad \times P\left(I_{\tau+1} \middle| I_0^\tau, J_0^{\tau+1}, \bigcup_{k=1}^K \mathcal{O}_{k,1}^{k,N}(\tau), \dots, \bigcup_{k=1}^K \mathcal{O}_{k,1}^{k,N}(0)\right) \\ &\quad \times P\left(J_{\tau+1} \middle| I_0^\tau, J_0^\tau, \bigcup_{k=1}^K \mathcal{O}_{k,1}^{k,N}(\tau), \dots, \bigcup_{k=1}^K \mathcal{O}_{k,1}^{k,N}(0)\right) \\ &\stackrel{5}{=} P\left(\bigcup_{k=1}^K \mathcal{O}_{k,1}^{k,N}(\tau+1) \middle| \bigcup_{k=1}^K \mathcal{O}_{k,1}^{k,N}(\tau), I_\tau, J_\tau\right) \times P(I_{\tau+1}) \times P(J_{\tau+1}), \end{aligned}$$

where in equality (1) we use the definition, in equality (2) we wrote the RB samples explicitly, in equality (3) the terms were rearranged, in equality (4) we expressed the probability as a conditional product, and in equality (5) we use the fact that I_τ and J_τ are independent random variables and the rule of pushing transition \mathcal{O}_τ into $RB(I_\tau)$:

$$\mathcal{O}_{t(k,1)}^{t(k,N)}(\tau+1) = \begin{cases} \mathcal{O}_{t(k,1)}^{t(k,N)}(\tau) & \text{if } k \neq I_\tau \\ \mathcal{O}_{t(k,1)}^{t(k,N-1)}(\tau) \cup \mathcal{O}_\tau & \text{if } k = I_\tau \end{cases}$$

Similarly, computing the r.h.s of (8) yields

$$\begin{aligned}
P(Y_{\tau+1}|Y_\tau) &= P\left(\bigcup_{k=1}^K RB_{\tau+1}(k), I_{\tau+1}, J_{\tau+1} \middle| \bigcup_{k=1}^K RB_\tau(k), I_\tau, J_\tau\right) \\
&= P\left(\bigcup_{k=1}^K RB_{\tau+1}(k) \middle| \bigcup_{k=1}^K RB_\tau(k), I_{\tau+1}, J_{\tau+1}, I_\tau, J_\tau\right) \\
&\quad \times P\left(I_{\tau+1} \middle| \bigcup_{k=1}^K RB_\tau(k), J_{\tau+1}, I_\tau, J_\tau\right) \times P\left(J_{\tau+1} \middle| \bigcup_{k=1}^K RB_\tau(k), I_\tau, J_\tau\right) \\
&= P\left(\bigcup_{k=1}^K RB_{\tau+1}(k) \middle| \bigcup_{k=1}^K RB_\tau(k), I_\tau, J_\tau\right) \times P(I_{\tau+1}) \times P(J_{\tau+1}) \\
&= P\left(\bigcup_{k=1}^K \mathcal{O}_{k,1}^{k,N}(\tau+1) \middle| \bigcup_{k=1}^K \mathcal{O}_{k,1}^{k,N}(\tau), I_\tau, J_\tau\right) \times P(I_{\tau+1}) \times P(J_{\tau+1}).
\end{aligned}$$

Both sides of (8) are equal and therefore Y_τ is Markovian.

2. According to Assumption 3, we assume that for every environment k and for every policy π the Markov Process induced by the MDP together with the policy π is irreducible and aperiodic. In addition, we assume $\tau \geq \tau'$, where τ' is the time where we have full K RBs, each one with N transitions. This means that when a new transition arrives to RB(k), it requires throwing away the oldest transition in the buffer. We saw in part **1** that

$$P(Y_{\tau+1}|Y_\tau) = P\left(\bigcup_{k=1}^K \mathcal{O}_{k,1}^{k,N}(\tau+1) \middle| \bigcup_{k=1}^K \mathcal{O}_{k,1}^{k,N}(\tau), I_\tau, J_\tau\right) \times P(I_{\tau+1}) \times P(J_{\tau+1}). \quad (9)$$

Let $\mathbb{K} = \{1, \dots, K\}$ be an index set. We now write explicitly the following term

$$\begin{aligned}
&P\left(\bigcup_{k=1}^K \mathcal{O}_{k,1}^{k,N}(\tau+1) \middle| \bigcup_{k=1}^K \mathcal{O}_{k,1}^{k,N}(\tau), I_\tau, J_\tau\right) \\
&= P\left(\underbrace{\mathcal{O}_{I_\tau,1}^{I_\tau,N}(\tau+1)}_{(a)} \middle| \bigcup_{k \in \mathbb{K} \setminus I_\tau} \mathcal{O}_{k,1}^{k,N}(\tau+1), \bigcup_{k=1}^K \mathcal{O}_{k,1}^{k,N}(\tau), I_\tau, J_\tau\right) \times P\left(\underbrace{\bigcup_{k \in \mathbb{K} \setminus I_\tau} \mathcal{O}_{k,1}^{k,N}(\tau+1) \middle| \bigcup_{k=1}^K \mathcal{O}_{k,1}^{k,N}(\tau), I_\tau, J_\tau}_{(b)}\right),
\end{aligned} \quad (10)$$

where we expressed the probability as a conditional product, separating RB(I_τ) at time $\tau+1$ from all other RB's. Note that in (b): $\mathcal{O}_{k,1}^{k,N}(\tau+1) = \mathcal{O}_{k,1}^{k,N}(\tau)$ for all $k \neq I_\tau$ since these RB's do not change in this time-step.

We continue with expression (a).

$$\begin{aligned}
&P\left(\mathcal{O}_{I_\tau,1}^{I_\tau,N}(\tau+1) \middle| \bigcup_{k \in \mathbb{K} \setminus I_\tau} \mathcal{O}_{k,1}^{k,N}(\tau+1), \bigcup_{k=1}^K \mathcal{O}_{k,1}^{k,N}(\tau), I_\tau, J_\tau\right) \\
&\stackrel{1}{=} P\left(\mathcal{O}_{I_\tau,1}^{I_\tau,N}(\tau+1) \middle| \mathcal{O}_{I_\tau,1}^{I_\tau,N}(\tau), I_\tau, J_\tau\right) \\
&\stackrel{2}{=} P(\mathcal{O}_{I_\tau,1}(\tau+1) | \mathcal{O}_{I_\tau,1}(\tau), I_\tau, J_\tau) \\
&\stackrel{3, (i=I_\tau, t_i=t_{I_\tau})}{=} P(s_{i,t_i}, a_{i,t_i}, r_{i,t_i}, s_{i,t_i+1} | s_{i,t_i-1}, a_{i,t_i-1}, r_{i,t_i-1}, s_{i,t_i}, I_\tau, J_\tau) \\
&\stackrel{4}{=} P(a_{i,t_i}, r_{i,t_i}, s_{i,t_i+1} | s_{i,t_i}, I_\tau, J_\tau) \\
&\stackrel{5}{=} P(r_{i,t_i}, s_{i,t_i+1} | s_{i,t_i}, a_{i,t_i}, I_\tau, J_\tau) \times P(a_{i,t_i} | s_{i,t_i}, I_\tau, J_\tau) \\
&\stackrel{6}{=} P(s_{i,t_i+1} | s_{i,t_i}, a_{i,t_i}, r_{i,t_i}, I_\tau, J_\tau) \times P(r_{i,t_i} | s_{i,t_i}, a_{i,t_i}) \times \pi_{\theta(J_\tau)}(a_{i,t_i} | s_{i,t_i}) \\
&\stackrel{7}{=} P_{I_\tau}^{\pi_{\theta(J_\tau)}}(s_{i,t_i+1} | s_{i,t_i}) \times P(r_{i,t_i} | s_{i,t_i}, a_{i,t_i})
\end{aligned} \quad (11)$$

where in equality (1) we omitted all $RB_{\tau+1}(k)$ and $RB_{\tau}(k)$ for $k \neq I_{\tau}$ since they do not influence $RB_{\tau+1}(I_{\tau})$ and for time τ we left only $RB_{\tau}(I_{\tau})$. For equality (2) we recall Remark 1: $\mathcal{O}_{k,n+1}(\tau+1) = \mathcal{O}_{k,n}(\tau)$ for $n = 1, \dots, N-1$ and $\mathcal{O}_{k,1}(\tau+1) = \mathcal{O}_{\tau}$. Therefore, the transitions which are equal in both sides of the probability in equality (1), can be omitted. In equality (3) we write the transitions explicitly and change the notation for easier readability, $i = I_{\tau}$ and $t_i = t_{I_{\tau}}$ where t_i is the last time-step in MDP M_i . In equality (4) we omit the condition of s_{i,t_i} on itself and we keep the conditions only on I_{τ} , J_{τ} and state s_{i,t_i} since the process $\{s_{i,t_i}\}_{t_i \geq 0}$ is Markovian. In equalities (5) and (6) we express the probability as a conditional product. We denoted the policy $\pi_{\theta(J_{\tau})}$ to emphasize that the policy depends on the observation sampled from $\text{RB}(J_{\tau})$. Observe that in our setup, both $P(r_{i,t_i}|s_{i,t_i}, a_{i,t_i})$ and $\pi_{\theta(J_{\tau})}(a_{i,t_i}|s_{i,t_i})$ are independent of I_{τ} . Finally, in equality (7) we use the transitions in the induced Markov processes $\{s_{i,t_i}\}_{t_i \geq 0}$, $P_{I_{\tau}}^{\pi_{\theta}}(s_{i,t_i+1}|s_{i,t_i}) = P_{I_{\tau}}(s_{i,t_i+1}|s_{i,t_i}, a_{i,t_i}) \times \pi_{\theta}(a_{i,t_i}|s_{i,t_i})$ (recall that we used $i = I_{\tau}$).

Recall that I_{τ} and J_{τ} are independent random variables and that $P(I_{\tau+1} = k) = q_k$ and $P(J_{\tau+1} = k) = \beta_k$. Combining (9), (10) and (11) yields

$$P(Y_{\tau+1}|Y_{\tau}) = P_{I_{\tau}}^{\pi_{\theta(J_{\tau})}}(s'|s) \times P(r|s, a) \times q_{I_{\tau+1}} \times \beta_{J_{\tau+1}}.$$

Using Assumption 3 and since the probability $P(r|s, a)$ does not influence the policy and MDP dynamics, the process Y_{τ} is aperiodic and irreducible. □

A.2 Proof of Theorem 2

Proof. Recall that our TD-error update in line 6 in Algorithm 1 is defined as $\delta(\tilde{\mathcal{O}}^z) = \tilde{r}^z - \eta + \phi(\tilde{s}'^z)^{\top} v - \phi(\tilde{s}^z)^{\top} v$, where $\tilde{\mathcal{O}}^z = \{\tilde{s}^z, \tilde{a}^z, \tilde{r}^z, \tilde{s}'^z\}$. In the critic update in line 8 in Algorithm 1 we use an empirical mean over several sampled observations, denoted as $\{\tilde{\mathcal{O}}^z\}_{z=1}^{N_{\text{samples}}}$. Then, the critic update is defined as

$$v' = v + \alpha^v \frac{1}{N_{\text{samples}}} \sum_z \delta(\tilde{\mathcal{O}}^z) \phi(\tilde{s}^z).$$

Consider $N_{\text{samples}} = 1$. For a single sample update, we will use the following notations for the rest of the proof: $\tilde{\mathcal{O}} = \{\tilde{s}, \tilde{a}, \tilde{r}, \tilde{s}'\}$ and $\delta(\tilde{\mathcal{O}}) = \tilde{r} - \eta + \phi(\tilde{s}')^{\top} v - \phi(\tilde{s})^{\top} v$.

In this proof we follow the proof of Lemma 5 in [5]. Observe that the average reward and critic updates from Algorithm 1 can be written as

$$\eta_{\tau+1} = \eta_{\tau} + \alpha_{\tau}^{\eta} (F_{\tau}^{\eta} + M_{\tau+1}^{\eta}) \tag{12}$$

$$v_{\tau+1} = v_{\tau} + \alpha_{\tau}^v (F_{\tau}^v + M_{\tau+1}^v), \tag{13}$$

where

$$\begin{aligned} F_{\tau}^{\eta} &\triangleq \mathbb{E}_{k \sim \beta, \tilde{\mathcal{O}} \sim \text{RB}(k), \tilde{s}, \tilde{a} \in \tilde{\mathcal{O}}} [\tilde{r} - \eta | \mathcal{F}_{\tau}] \\ M_{\tau+1}^{\eta} &\triangleq (\tilde{r} - \eta_{\tau}) - F_{\tau}^{\eta} \\ F_{\tau}^v &\triangleq \mathbb{E}_{k \sim \beta, \tilde{\mathcal{O}} \sim \text{RB}(k), \tilde{s}, \tilde{a}, \tilde{s}' \in \tilde{\mathcal{O}}} [\delta(\tilde{\mathcal{O}}) \phi(\tilde{s}) | \mathcal{F}_{\tau}] \\ M_{\tau+1}^v &\triangleq \delta(\tilde{\mathcal{O}}) \phi(\tilde{s}) - F_{\tau}^v \end{aligned}$$

and \mathcal{F}_{τ} is a σ -algebra defined as $\mathcal{F}_{\tau} \triangleq \{\eta_t, v_t, M_t^{\eta}, M_t^v : t \leq \tau\}$.

We use Theorem 2.2 of [9] to prove convergence of these iterates. Briefly, this theorem states that given an iteration as in (12) and (13), these iterations are bounded w.p.1 if

Assumption 8. 1. F_{τ}^{η} and F_{τ}^v are Lipschitz, the functions $F_{\infty}^{\eta}(\eta) = \lim_{\sigma \rightarrow \infty} F_{\tau}^{\eta}(\sigma\eta)/\sigma$ and $F_{\infty}^v(v) = \lim_{\sigma \rightarrow \infty} F_{\tau}^v(\sigma v)/\sigma$ are Lipschitz, and $F_{\infty}^{\eta}(\eta)$ and $F_{\infty}^v(v)$ are asymptotically stable in the origin.

2. The sequences $M_{\tau+1}^{\eta}$ and $M_{\tau+1}^v$ are martingale difference noises and for some C_0^{η}, C_0^v

$$\mathbb{E} [(M_{\tau+1}^{\eta})^2 | \mathcal{F}_{\tau}] \leq C_0^{\eta} (1 + \|\eta_{\tau}\|^2)$$

$$\mathbb{E} [(M_{\tau+1}^v)^2 | \mathcal{F}_{\tau}] \leq C_0^v (1 + \|v_{\tau}\|^2).$$

We begin with the average reward update in (12). The ODE describing its asymptotic behavior corresponds to

$$\dot{\eta} = \mathbb{E}_{k \sim \beta, \tilde{\mathcal{O}} \sim \text{RB}(k), \tilde{s}, \tilde{a} \in \tilde{\mathcal{O}}} [\tilde{r} - \eta] \triangleq F^\eta. \quad (14)$$

F^η is Lipschitz continuous in η . The function $F_\infty(\eta)$ exists and satisfies $F_\infty(\eta) = -\eta$. The origin is an asymptotically stable equilibrium for the ODE $\dot{\eta} = F_\infty(\eta)$ and the related Lyapunov function is given by $\eta^2/2$.

For the critic update, consider the ODE

$$\dot{v} = \mathbb{E}_{k \sim \beta, \tilde{\mathcal{O}} \sim \text{RB}(k), \tilde{s}, \tilde{a}, \tilde{s}' \in \tilde{\mathcal{O}}} \left[\delta(\tilde{\mathcal{O}}) \phi(\tilde{s}) \right] \triangleq F^v$$

In Lemma 5 we show that this ODE can be written as

$$\dot{v} = \Phi^\top A_\theta \Phi v + \Phi^\top b_\theta, \quad (15)$$

where A_θ and b_θ are defined in (7). F^v is Lipschitz continuous in v and $F_\infty(v)$ exists and satisfies $F_\infty(v) = \Phi^\top A_\theta \Phi v$. Consider the system

$$\dot{v} = F_\infty(v) \quad (16)$$

In assumption 5 we assume that $\Phi v \neq e$ for every $v \in \mathbb{R}^d$. Therefore, the only asymptotically stable equilibrium for (16) is the origin (see the explanation in the proof of Lemma 5 in [5]). Therefore, for all $\tau \geq 0$

$$\mathbb{E} [(M_{\tau+1}^\eta)^2 | \mathcal{F}_\tau] \leq C_0^\eta (1 + \|\eta_\tau\|^2 + \|v_\tau\|^2)$$

$$\mathbb{E} [(M_{\tau+1}^v)^2 | \mathcal{F}_\tau] \leq C_0^v (1 + \|\eta_\tau\|^2 + \|v_\tau\|^2)$$

for some $C_0^\eta, C_0^v < \infty$. M_τ^η can be directly seen to be uniformly bounded almost surely. Thus, Assumptions (A1) and (A2) of [9] are satisfied for the average reward, TD-error, and critic updates. From Theorem 2.1 of [9], the average reward, TD-error, and critic iterates are uniformly bounded with probability one. Note that when $\tau \rightarrow \infty$, (14) has $\bar{\eta}_\theta$ defined as in (3) as its unique globally asymptotically stable equilibrium with $V_2(\eta) = (\eta - \bar{\eta}_\theta)^2$ serving as the associated Lyapunov function.

Next, suppose that $v = v^\pi$ is a solution to the system $\Phi^\top A_\theta \Phi v = 0$. Under Assumption 5, using the same arguments as in the proof of Lemma 5 in [5], v^π is the unique globally asymptotically stable equilibrium of the ODE (15). Assumption 8 is now verified and under Assumption 6, the claim follows from Theorem 2.2, pp. 450 of [9].

□

A.2.1 Auxiliary Lemma for Theorem 2

The following Lemma computes the expectation of the critic update $\mathbb{E} [\delta(\tilde{\mathcal{O}}) \phi(\tilde{s})]$.

Lemma 5. *Assume we have full K RBs, each one with N transitions. Then the following holds*

$$\mathbb{E}_{k \sim \beta, \tilde{\mathcal{O}} \sim \text{RB}(k), \tilde{s}, \tilde{a}, \tilde{s}' \in \tilde{\mathcal{O}}} \left[\delta(\tilde{\mathcal{O}}) \phi(\tilde{s}) \right] = \Phi^\top A_\theta \Phi v + \Phi^\top b_\theta,$$

where A_θ and b_θ are defined in (7).

Proof. We note that due to the probabilistic nature of Algorithm 1, we do not know explicitly when each sample was pushed to any of the RBs. Next, we compute the expectation of the critic update with linear function approximation according to Algorithm 1.

$$\begin{aligned}
& \mathbb{E}_{k \sim \beta, \tilde{\mathcal{O}} \sim \text{RB}(k), \tilde{s}, \tilde{a}, \tilde{s}' \in \tilde{\mathcal{O}}} \left[\delta(\tilde{\mathcal{O}}) \phi(\tilde{s}) \right] \\
&= \mathbb{E}_{k \sim \beta, \tilde{\mathcal{O}} \sim \text{RB}(k), \tilde{s}, \tilde{a}, \tilde{s}' \in \tilde{\mathcal{O}}} \left[(r(\tilde{s}, \tilde{a}) - \eta + \phi(\tilde{s}')^\top v - \phi(\tilde{s})^\top v) \phi(\tilde{s}) \right] \\
&= \mathbb{E}_{k \sim \beta} \left[\mathbb{E}_{\tilde{\mathcal{O}} \sim \text{RB}(k), \tilde{s}, \tilde{a}, \tilde{s}' \in \tilde{\mathcal{O}}} \left[(r(\tilde{s}, \tilde{a}) - \eta + \phi(\tilde{s}')^\top v - \phi(\tilde{s})^\top v) \phi(\tilde{s}) \right] \right] \\
&= \sum_{k=1}^K \beta_k \mathbb{E}_{\tilde{\mathcal{O}} \sim \text{RB}(k), \tilde{s}, \tilde{a}, \tilde{s}' \in \tilde{\mathcal{O}}} \left[(r(\tilde{s}, \tilde{a}) - \eta + \phi(\tilde{s}')^\top v - \phi(\tilde{s})^\top v) \phi(\tilde{s}) \right] \quad (17) \\
&= \sum_{k=1}^K \beta_k \mathbb{E}_{\tilde{\mathcal{O}} \sim \text{RB}(k)} \left[\mathbb{E}_{\tilde{s}, \tilde{a}, \tilde{s}' \in \tilde{\mathcal{O}}_k} \left[(r(\tilde{s}, \tilde{a}) - \eta + \phi(\tilde{s}')^\top v - \phi(\tilde{s})^\top v) \phi(\tilde{s}) \right] \right] \\
&= \sum_{k=1}^K \beta_k \sum_{n=1}^N \frac{1}{N} \mathbb{E}_{\tilde{s}, \tilde{a}, \tilde{s}' \in \tilde{\mathcal{O}}_{k,n}} \left[(r(\tilde{s}, \tilde{a}) - \eta + \phi(\tilde{s}')^\top v - \phi(\tilde{s})^\top v) \phi(\tilde{s}) \right].
\end{aligned}$$

We note that in the last expression, the inner expectation is according to a tuple of indices (k, n) where k corresponds to $\text{RB}(k)$ and n corresponds to the n -th transition in this $\text{RB}(k)$. Also, this sample (k, n) corresponds to some $\theta_{t(k,n)}$. Recall that the time $t(k, n)$ is the time that the agent interacted with the k -th MDP and since then n samples were added to $\text{RB}(k)$ (and the n oldest samples were removed). In other words, sample $(k, n = 1)$ is the newest sample in $\text{RB}(k)$ while sample $(k, n = N)$ is the oldest. Abusing notation, we define

$$t(k, n) = \{t \mid \text{For the time } \tau, \text{ the time } t \text{ the } n\text{-th sample in } \text{RB}(k) \text{ was pushed.}\} \quad (18)$$

Next, we define the induced MC for the time $t(k, n)$ with a corresponding parameter $\theta_{t(k,n)}$. For this parameter, we denote the corresponding state distribution vector $\rho_{t(k,n)}$ and a transition matrix $P_{t(k,n)}$ (both induced by the policy $\pi_{\theta_{t(k,n)}}$). In addition, we define the following diagonal matrix $S_{t(k,n)} \triangleq \text{diag}(\rho_{t(k,n)})$. Similarly to [4] Lemma 6.5, pp.298, we can substitute the inner expectation

$$\begin{aligned}
& \mathbb{E}_{\tilde{s}, \tilde{a}, \tilde{s}' \in \tilde{\mathcal{O}}_{k,n}} \left[(r(\tilde{s}, \tilde{a}) - \eta + \phi(\tilde{s}')^\top v - \phi(\tilde{s})^\top v) \phi(\tilde{s}) \right] = \\
& \Phi^\top S_{t(k,n)} (P_{t(k,n)} - I) \Phi v + \Phi^\top S_{t(k,n)} (r_{t(k,n)} - \eta_{\theta,k} e),
\end{aligned} \quad (19)$$

where I is the $|\mathcal{S}| \times |\mathcal{S}|$ identity matrix, e in $|\mathcal{S}| \times 1$ vector of ones and $r_{k,n}$ is a $|\mathcal{S}| \times 1$ vector defined as $r_{t(k,n)}(s) = \sum_a \pi_{\theta_{t(k,n)}}(a|s) r(s, a)$. Combining equations (6), (17) and (19) yields

$$\sum_{k=1}^K \sum_{n=1}^N \frac{\beta_k}{N} (\Phi^\top S_{t(k,n)} (P_{t(k,n)} - I) \Phi v + \Phi^\top S_{t(k,n)} (r_{t(k,n)} - \eta_{\theta,k} e)) = \Phi^\top A_\tau \Phi v + \Phi^\top b_\tau, \quad (20)$$

In the limit, $\tau \rightarrow \infty$ and $\rho_{t(k,n)} \rightarrow \mu_{\theta,k}$ for all index n . Using A_θ and b_θ defined in (7), (17) can be expressed as

$$\mathbb{E}_{k \sim \beta, \tilde{\mathcal{O}} \sim \text{RB}(k), \tilde{s}, \tilde{a}, \tilde{s}' \in \tilde{\mathcal{O}}} \left[\delta(\tilde{\mathcal{O}}) \phi(\tilde{s}) \right] = \Phi^\top A_\theta \Phi v + \Phi^\top b_\theta. \quad (21)$$

□

A.3 Proof of Theorem 3

Proof. Recall that our TD-error update in line 6 in Algorithm 1 is defined as $\delta(\tilde{\mathcal{O}}^z) = \tilde{r}^z - \eta + \phi(\tilde{s}'^z)^\top v - \phi(\tilde{s}^z)^\top v$, where $\tilde{\mathcal{O}}^z = \{\tilde{s}^z, \tilde{a}^z, \tilde{r}^z, \tilde{s}'^z\}$. In the actor update in line 9 in Algorithm 1 we use an empirical mean over several sampled observations, denoted as $\{\tilde{\mathcal{O}}^z\}_{z=1}^{N_{\text{samples}}}$. Then, the actor update is defined as

$$\theta' = \Gamma \left(\theta - \alpha^\theta \frac{1}{N_{\text{samples}}} \sum_z \delta(\tilde{\mathcal{O}}^z) \nabla \log \pi_\theta(\tilde{a}^z | \tilde{s}^z) \right).$$

Consider $N_{\text{samples}} = 1$. For a single sample update, we will use the following notations for the rest of the proof: $\tilde{\mathcal{O}} = \{\tilde{s}, \tilde{a}, \tilde{r}, \tilde{s}'\}$ and $\delta(\tilde{\mathcal{O}}) = \tilde{r} - \eta + \phi(\tilde{s}')^\top v - \phi(\tilde{s})^\top v$.

In this proof we follow the proof of Theorem 2 in [5]. Let $\delta^\pi(\tilde{\mathcal{O}}) = \tilde{r} - \eta + \phi(\tilde{s}')^\top v^\pi - \phi(\tilde{s})^\top v^\pi$, where v^π is the convergent parameter of the critic recursion with probability one (see its definition in the proof for Theorem 2). Observe that the actor parameter update from Algorithm 1 can be written as

$$\begin{aligned}\theta_{\tau+1} &= \Gamma\left(\theta_\tau - \alpha_\tau^\theta (\delta(\tilde{\mathcal{O}}) \nabla_\theta \log \pi_\theta(\tilde{a}|\tilde{s}) + F_\tau^\theta - F_\tau^\theta + N_\tau^{\theta\tau} - N_\tau^{\theta\tau})\right) \\ &= \Gamma\left(\theta_\tau - \alpha_\tau^\theta (M_{\tau+1}^\theta + (F_\tau^\theta - N_\tau^{\theta\tau}) + N_\tau^{\theta\tau})\right)\end{aligned}$$

where

$$\begin{aligned}F_\tau^\theta &\triangleq \mathbb{E}_{k \sim \beta, \tilde{\mathcal{O}} \sim \text{RB}(k), \tilde{a}, \tilde{s}, \tilde{s}' \in \tilde{\mathcal{O}}} \left[\delta(\tilde{\mathcal{O}}) \nabla_\theta \log \pi_\theta(\tilde{a}|\tilde{s}) \middle| \mathcal{F}_\tau \right] \\ M_{\tau+1}^\theta &\triangleq \delta(\tilde{\mathcal{O}}) \nabla_\theta \log \pi_\theta(\tilde{a}|\tilde{s}) - F_\tau^\theta \\ N_\tau^\theta &\triangleq \mathbb{E}_{k \sim \beta, \tilde{\mathcal{O}} \sim \text{RB}(k), \tilde{s}, \tilde{a}, \tilde{s}' \in \tilde{\mathcal{O}}} \left[\delta^{\pi_\theta}(\tilde{\mathcal{O}}) \nabla_\theta \log \pi_\theta(\tilde{a}|\tilde{s}) \middle| \mathcal{F}_\tau \right]\end{aligned}$$

and \mathcal{F}_τ is a σ -algebra defined as $\mathcal{F}_\tau \triangleq \{\eta_t, v_t, \theta_t, M_t^\eta, M_t^v, M_t^\theta : t \leq \tau\}$.

Since the critic converges along the faster timescale, from Theorem 2 it follows that $F_\tau^\theta - N_\tau^{\theta\tau} = o(1)$. Now, let

$$M_2(\tau) = \sum_{r=0}^{\tau-1} \alpha_r^\theta M_{r+1}^\theta, \tau \geq 1.$$

The quantities $\delta(\tilde{\mathcal{O}})$ can be seen to be uniformly bounded since from the proof in Theorem 2, $\{\eta_\tau\}$ and $\{v_\tau\}$ are bounded sequences. Therefore, using Assumption 6, $\{M_2(\tau)\}$ is a convergent martingale sequence [6].

Consider the actor update along the slower timescale corresponding to α_τ^θ in line (9) in Algorithm 1. Let $v(\cdot)$ be a vector field on a set Θ . Define another vector field: $\hat{\Gamma}(v(y)) = \lim_{0 < \eta \rightarrow 0} = \left(\frac{\Gamma(y + \eta v(y)) - y}{\eta} \right)$. In case this limit is not unique, we let $\hat{\Gamma}(v(y))$ be the set of all possible limit points (see pp. 191 of [28]). Consider now the ODE

$$\dot{\theta} = \hat{\Gamma}\left(-\mathbb{E}_{k \sim \beta, \tilde{\mathcal{O}} \sim \text{RB}(k), \tilde{s}, \tilde{a}, \tilde{s}' \in \tilde{\mathcal{O}}} \left[\delta^{\pi_\theta}(\tilde{\mathcal{O}}) \nabla_\theta \log \pi_\theta(\tilde{a}|\tilde{s}) \right]\right) \quad (22)$$

Substituting the result from Lemma 6, the above ODE is analogous to

$$\dot{\theta} = \hat{\Gamma}(-\nabla_\theta \bar{\eta}_\theta + \xi^{\pi_\theta}) = \hat{\Gamma}(-N_\tau^\theta) \quad (23)$$

where $\xi^{\pi_\theta} = \sum_{k=1}^K \beta_k \sum_{\tilde{s}} \mu_{\theta,k}(\tilde{s}) \left(\phi(\tilde{s})^\top \nabla_\theta v^{\pi_\theta} - \nabla_\theta \bar{V}_k^{\pi_\theta}(\tilde{s}) \right)$. Consider also an associated ODE:

$$\dot{\theta} = \hat{\Gamma}(-\nabla_\theta \bar{\eta}_\theta) \quad (24)$$

We now show that $h_1(\theta_\tau) \triangleq -N_\tau^{\theta\tau}$ is Lipschitz continuous. Here $v^{\pi_{\theta_\tau}}$ corresponds to the weight vector to which the critic update converges along the faster timescale when the corresponding policy is π_{θ_τ} (see Theorem 2). Note that $\mu_{\theta,k}(s), s \in \mathcal{S}, k \in \{1, \dots, K\}$ are continuously differentiable in θ and have bounded derivatives. Also, $\bar{\eta}_{\theta_\tau}$ is continuously differentiable as well and has bounded derivative as can also be seen from (1). Further, $v^{\pi_{\theta_\tau}}$ can be seen to be continuously differentiable with bounded derivatives. Finally, $\nabla^2 \pi_{\theta_\tau}(a|s)$ exists and is bounded. Thus $h_1(\theta_\tau)$ is a Lipschitz continuous function and the ODE (22) is well posed.

Let \mathcal{Z} denote the set of asymptotically stable equilibria of (24) i.e., the local minima of $\bar{\eta}_\theta$, and let \mathcal{Z}^ϵ be the ϵ -neighborhood of \mathcal{Z} . To complete the proof, we are left to show that as $\sup_\theta \|\xi^{\pi_\theta}\| \rightarrow 0$ (viz. $\delta \rightarrow 0$), the trajectories of (23) converge to those of (24) uniformly on compacts for the same initial condition in both. This claim follows the same arguments as in the proof of Theorem 2 in [5].

□

A.3.1 Auxiliary Lemma for Theorem 3

The following Lemma computes the expectation of $\mathbb{E} \left[\delta^{\pi_\theta}(\tilde{\mathcal{O}}) \nabla_\theta \log \pi_\theta(\tilde{a}|\tilde{s}) \right]$.

Lemma 6. *Assume we have full K RBs, each one with N transitions. Then the following holds*

$$\begin{aligned} & \mathbb{E}_{k \sim \beta, \tilde{\mathcal{O}} \sim \text{RB}(k), \tilde{s}, \tilde{a}, \tilde{s}' \in \tilde{\mathcal{O}}} \left[\delta^{\pi_\theta}(\tilde{\mathcal{O}}) \nabla_\theta \log \pi_\theta(\tilde{a}|\tilde{s}) \right] \\ &= \nabla_\theta \bar{\eta}_\theta - \sum_{k=1}^K \beta_k \sum_{\tilde{s}} \mu_{\theta,k}(\tilde{s}) \left(\phi(\tilde{s})^\top \nabla_\theta v^{\pi_\theta} - \nabla_\theta \bar{V}_k^{\pi_\theta}(\tilde{s}) \right), \end{aligned}$$

where $\bar{V}_k^{\pi_\theta}(\tilde{s}) = \sum_{\tilde{a} \in \mathcal{A}} \pi_\theta(\tilde{a}|\tilde{s}) \left(r(\tilde{s}, \tilde{a}) - \eta_{\theta,k} + \sum_{\tilde{s}' \in \mathcal{S}} P_k(\tilde{s}'|\tilde{s}, \tilde{a}) \phi(\tilde{s}')^\top v^{\pi_\theta} \right)$.

Proof. We compute the expectation of $\delta^{\pi_\theta}(\tilde{\mathcal{O}}) \nabla_\theta \log \pi_\theta(\tilde{a}|\tilde{s})$ with linear function approximation according to Algorithm 1. Due to the probabilistic nature of Algorithm 1, we do not know explicitly when each transition was pushed to any of the RBs. Recall that the tuple (k, n) corresponds to some $\theta_{t(k,n)}$ where time $t(k, n)$ was defined in Section 4. We use the same notations for the state distribution vector $\rho_{t(k,n)}$ and a transition matrix $P_{t(k,n)}$ (both induced by the policy $\pi_{\theta_{t(k,n)}}$, as in the proof for Lemma 5). We define now the following term:

$$\bar{V}_k^{\pi_{\theta_{t(k,n)}}}(\tilde{s}) = \sum_{\tilde{a} \in \mathcal{A}} \pi_{\theta_{t(k,n)}}(\tilde{a}|\tilde{s}) \bar{Q}_k^{\pi_{\theta_{t(k,n)}}}(\tilde{s}, \tilde{a}) = \sum_{\tilde{a} \in \mathcal{A}} \pi_{\theta_{t(k,n)}}(\tilde{a}|\tilde{s}) \left(r(\tilde{s}, \tilde{a}) - \eta_{\theta,k} + \sum_{\tilde{s}' \in \mathcal{S}} P_k(\tilde{s}'|\tilde{s}, \tilde{a}) \phi(\tilde{s}')^\top v^{\pi_\theta} \right), \quad (25)$$

where $\bar{V}_k^{\pi_{\theta_{t(k,n)}}}(\tilde{s})$ and $\bar{Q}_k^{\pi_{\theta_{t(k,n)}}}(\tilde{s}, \tilde{a})$ correspond to policy $\pi_{\theta_{t(k,n)}}$. Note that here, the convergent critic parameter v^{π_θ} is used. Let's look at the gradient of (25):

$$\begin{aligned} \nabla_\theta \bar{V}_k^{\pi_{\theta_{t(k,n)}}}(\tilde{s}) &= \nabla_\theta \left(\sum_{\tilde{a} \in \mathcal{A}} \pi_{\theta_{t(k,n)}}(\tilde{a}|\tilde{s}) \bar{Q}_k^{\pi_{\theta_{t(k,n)}}}(\tilde{s}, \tilde{a}) \right) \\ &= \sum_{\tilde{a} \in \mathcal{A}} \nabla_\theta \pi_{\theta_{t(k,n)}}(\tilde{a}|\tilde{s}) \left(r(\tilde{s}, \tilde{a}) - \eta_{\theta,k} + \sum_{\tilde{s}' \in \mathcal{S}} P_k(\tilde{s}'|\tilde{s}, \tilde{a}) \phi(\tilde{s}')^\top v^{\pi_\theta} \right) \\ &\quad + \sum_{\tilde{a} \in \mathcal{A}} \pi_{\theta_{t(k,n)}}(\tilde{a}|\tilde{s}) \left(-\nabla_\theta \eta_{\theta,k} + \sum_{\tilde{s}' \in \mathcal{S}} P_k(\tilde{s}'|\tilde{s}, \tilde{a}) \phi(\tilde{s}')^\top \nabla_\theta v^{\pi_\theta} \right) \\ &= \sum_{\tilde{a} \in \mathcal{A}} \nabla_\theta \pi_{\theta_{t(k,n)}}(\tilde{a}|\tilde{s}) \left(r(\tilde{s}, \tilde{a}) - \eta_{\theta,k} + \sum_{\tilde{s}' \in \mathcal{S}} P_k(\tilde{s}'|\tilde{s}, \tilde{a}) \phi(\tilde{s}')^\top v^{\pi_\theta} \right) \\ &\quad - \nabla_\theta \eta_{\theta,k} + \sum_{\tilde{a} \in \mathcal{A}} \pi_{\theta_{t(k,n)}}(\tilde{a}|\tilde{s}) \sum_{\tilde{s}' \in \mathcal{S}} P_k(\tilde{s}'|\tilde{s}, \tilde{a}) \phi(\tilde{s}')^\top \nabla_\theta v^{\pi_\theta} \end{aligned}$$

where with abuse of notation, $\nabla_\theta \pi_{\theta_{t(k,n)}}(\tilde{a}|\tilde{s}) = \nabla_\theta \pi_{\theta|\theta=\theta_{t(k,n)}}(\tilde{a}|\tilde{s})$. In the limit, $\tau \rightarrow \infty$ and $\rho_{t(k,n)} \rightarrow \mu_{\theta,k}$ for all index n . Summing both sides over β distribution and stationary distribution $\mu_{\theta,k}$

$$\begin{aligned} & \sum_{k=1}^K \beta_k \sum_{\tilde{s}} \mu_{\theta,k}(\tilde{s}) \nabla_\theta \bar{V}_k^{\pi_\theta}(\tilde{s}) \\ &= \sum_{k=1}^K \beta_k \sum_{\tilde{s}} \mu_{\theta,k}(\tilde{s}) \sum_{\tilde{a} \in \mathcal{A}} \nabla_\theta \pi_\theta(\tilde{a}|\tilde{s}) \left(r(\tilde{s}, \tilde{a}) - \eta_{\theta,k} + \sum_{\tilde{s}' \in \mathcal{S}} P_k(\tilde{s}'|\tilde{s}, \tilde{a}) \phi(\tilde{s}')^\top v^{\pi_\theta} \right) \\ &\quad + \sum_{k=1}^K \beta_k \sum_{\tilde{s}} \mu_{\theta,k}(\tilde{s}) \left(-\nabla_\theta \eta_{\theta,k} + \sum_{\tilde{a} \in \mathcal{A}} \pi_\theta(\tilde{a}|\tilde{s}) \sum_{\tilde{s}' \in \mathcal{S}} P_k(\tilde{s}'|\tilde{s}, \tilde{a}) \phi(\tilde{s}')^\top \nabla_\theta v^{\pi_\theta} \right) \\ &= \mathbb{E}_{k \sim \beta, \tilde{\mathcal{O}} \sim \text{RB}(k), \tilde{s}, \tilde{a}, \tilde{s}' \in \tilde{\mathcal{O}}} \left[\delta^{\pi_\theta}(\tilde{\mathcal{O}}) \nabla_\theta \log \pi_\theta(\tilde{a}|\tilde{s}) \right] \\ &\quad - \nabla_\theta \bar{\eta}_\theta + \sum_{k=1}^K \beta_k \sum_{\tilde{s}} \mu_{\theta,k}(\tilde{s}) \sum_{\tilde{a} \in \mathcal{A}} \pi_\theta(\tilde{a}|\tilde{s}) \sum_{\tilde{s}' \in \mathcal{S}} P_k(\tilde{s}'|\tilde{s}, \tilde{a}) \phi(\tilde{s}')^\top \nabla_\theta v^{\pi_\theta} \end{aligned}$$

We will write in short $\mathbb{E} \left[\delta^{\pi_\theta}(\tilde{\mathcal{O}}) \nabla_\theta \log \pi_\theta(\tilde{a}|\tilde{s}) \right] = \mathbb{E}_{k \sim \beta, \tilde{\mathcal{O}} \sim \text{RB}(k), \tilde{s}, \tilde{a}, \tilde{s}' \in \tilde{\mathcal{O}}} \left[\delta^{\pi_\theta}(\tilde{\mathcal{O}}) \nabla_\theta \log \pi_{\theta_{t(k,i)}}(\tilde{a}|\tilde{s}) \right]$.

Then:

$$\begin{aligned} \nabla_\theta \bar{\eta}_\theta &= \mathbb{E} \left[\delta^{\pi_\theta}(\tilde{\mathcal{O}}) \nabla_\theta \log \pi_\theta(\tilde{a}|\tilde{s}) \right] \\ &+ \sum_{k=1}^K \beta_k \sum_{\tilde{s}} \mu_{\theta,k}(\tilde{s}) \left(\sum_{\tilde{a} \in \mathcal{A}} \pi_\theta(\tilde{a}|\tilde{s}) \sum_{\tilde{s}' \in \mathcal{S}} P_k(\tilde{s}'|\tilde{s}, \tilde{a}) \phi(\tilde{s}')^\top \nabla_\theta v^{\pi_\theta} - \nabla_\theta \bar{V}_k^{\pi_\theta}(\tilde{s}) \right). \end{aligned}$$

Since $\mu_{\theta,k}$ is the stationary distribution for each environment k ,

$$\begin{aligned} \sum_{\tilde{s}} \mu_{\theta,k}(\tilde{s}) \sum_{\tilde{a} \in \mathcal{A}} \pi_\theta(\tilde{a}|\tilde{s}) \sum_{\tilde{s}' \in \mathcal{S}} P_k(\tilde{s}'|\tilde{s}, \tilde{a}) \phi(\tilde{s}')^\top \nabla_\theta v^{\pi_\theta} &= \sum_{\tilde{s}} \mu_{\theta,k}(\tilde{s}) \sum_{\tilde{s}' \in \mathcal{S}} P_{\theta,k}(\tilde{s}'|\tilde{s}) \phi(\tilde{s}')^\top \nabla_\theta v^{\pi_\theta} \\ &= \sum_{\tilde{s}'} \sum_{\tilde{s}} \mu_{\theta,k}(\tilde{s}) P_{\theta,k}(\tilde{s}'|\tilde{s}) \phi(\tilde{s}')^\top \nabla_\theta v^{\pi_\theta} \\ &= \sum_{\tilde{s}'} \mu_{\theta,k}(\tilde{s}') \phi(\tilde{s}')^\top \nabla_\theta v^{\pi_\theta}, \end{aligned}$$

Then,

$$\nabla_\theta \bar{\eta}_\theta = \mathbb{E} \left[\delta^{\pi_\theta}(\tilde{\mathcal{O}}) \nabla_\theta \log \pi_\theta(\tilde{a}|\tilde{s}) \right] + \sum_{k=1}^K \beta_k \sum_{\tilde{s}} \mu_{\theta,k}(\tilde{s}) \left(\phi(\tilde{s})^\top \nabla_\theta v^{\pi_\theta} - \nabla_\theta \bar{V}_k^{\pi_\theta}(\tilde{s}) \right)$$

The result follows immediately. □

B Proof of Main Lemmas and Theorems of Section 5.2

B.1 Proof of Theorem 4

Proof. **1.** We have a common policy to both sim and real. Thus,

$$\begin{aligned} |P_s^\theta(s'|s) - P_r^\theta(s'|s)| &= \left| \sum_{a \in \mathcal{A}} P_s(s'|s, a) \pi_\theta(a|s) - \sum_{a \in \mathcal{A}} P_r(s'|s, a) \pi_\theta(a|s) \right| \\ &= \left| \sum_{a \in \mathcal{A}} \pi_\theta(a|s) (P_s(s'|s, a) - P_r(s'|s, a)) \right| \\ &\leq \sum_{a \in \mathcal{A}} \pi_\theta(a|s) |P_s(s'|s, a) - P_r(s'|s, a)| \\ &\leq |A| \epsilon_{s2r}, \end{aligned} \tag{26}$$

where the last inequality is due to Assumption 7.

2. The stationary distribution satisfies $\mu_s^{\theta \top} P_s^\theta = \mu_s^{\theta \top}$. Let us define $\Delta P \triangleq P_s^\theta - P_r^\theta$ and $\Delta \mu \triangleq \mu_s^\theta - \mu_r^\theta$. Then, we have

$$\begin{aligned} \mu_s^{\theta \top} (P_s^\theta - I) &= 0 \\ (\mu_r^\theta + \Delta \mu)^\top (P_s^\theta - I) &= 0 \\ \mu_r^{\theta \top} (P_s^\theta - I) + \Delta \mu^\top (P_s^\theta - I) &= 0 \\ \mu_r^{\theta \top} (\Delta P + P_r^\theta - I) + \Delta \mu^\top (P_s^\theta - I) &= 0 \\ \mu_r^{\theta \top} (P_r^\theta - I) + \mu_r^{\theta \top} \Delta P + \Delta \mu^\top (P_s^\theta - I) &= 0 \\ \mu_r^{\theta \top} \Delta P + \Delta \mu^\top (P_s^\theta - I) &= 0 \\ \Delta \mu^\top (P_s^\theta - I) &= -\mu_r^{\theta \top} \Delta P. \end{aligned} \tag{27}$$

We note that since P_s^θ satisfies Assumption 2, it is of degree $|S| - 1$ (P_s^θ has only one eigenvalue equals 1, thus, $I - P_s^\theta$ has only one eigenvalue equals 0). Without loss of generality, we define $\tilde{\Delta}\mu$ to be a vector with the first $|S| - 1$ entries, \tilde{P}_s^θ to be a sub-matrix with the first $(|S| - 1) \times (|S| - 1)$ entries of P_s^θ , $\tilde{\mu}_r^\theta$ a vector with the first $|S| - 1$ first entries of μ_r^θ , $\tilde{\Delta}P$ a sub-matrix with the first $(|S| - 1) \times (|S| - 1)$ entries of ΔP , and \tilde{I} to be identity matrix of dimension $S - 1$. As a result, we have the following full rank equations system:

$$\tilde{\Delta}\mu \left(\tilde{P}_s^\theta - I \right) = -\tilde{\mu}_r^{\theta \top} \tilde{\Delta}P, \quad (28)$$

and the matrix $\left(\tilde{P}_s^\theta - I \right)$ is of full rank and invertible. Thus,

$$\tilde{\Delta}\mu = -\tilde{\mu}_r^{\theta \top} \tilde{\Delta}P \left(\tilde{P}_s^\theta - I \right)^{-1}. \quad (29)$$

We apply the Frobenius norm on both sides and get

$$\begin{aligned} \|\tilde{\Delta}\mu\|_F &= \left\| \tilde{\mu}_r^{\theta \top} \tilde{\Delta}P \left(\tilde{P}_s^\theta - I \right)^{-1} \right\|_F. \\ &\leq \left\| \tilde{\mu}_r^\theta \right\|_F \left\| \tilde{\Delta}P \right\|_F \left\| \left(\tilde{P}_s^\theta - I \right)^{-1} \right\|_F. \\ &\leq 1 \cdot |S|^2 \cdot \epsilon \left\| \left(\tilde{P}_s^\theta - I \right)^{-1} \right\|_F. \end{aligned} \quad (30)$$

We note that according to Assumption 1, Θ is compact and according to Assumption 3 the induced MC is aperiodic and irreducible. Therefore, the Frobenius norm of the latter norm (for all $\theta \in \Theta$) gets both the maximum and the minimum in Θ . Using Gersgorin Theorem ([18]; Thrm 6.1.1) on matrix $\tilde{P}_s^\theta - I$, and since the diagonal is greater than 1 and for each row, the off diagonal entries sum to less than 1, all the eigenvalues of $\tilde{P}_s^\theta - I$ are strictly above some value $R_G > 0$. As a result, the eigenvalues of $\left(\tilde{P}_s^\theta - I \right)^{-1}$ are bounded by R_G^{-1} . Using Assumption 3, the matrix $\left(\tilde{P}_s^\theta \right)^{-1}$ is bounded for all $\theta \in \Theta$ by $R_M \triangleq \max_{\theta \in \Theta} R_G^{-1}$, and the Frobenius of the latter norm is bounded by $\sqrt{S \cdot R_M}$. Summarizing, $\|\tilde{\Delta}\mu\| \leq \epsilon |S|^2 \min_{\theta \in \Theta} \sqrt{S R_M^2}$ for the first $S - 1$ states. We left with proving that for the last state, the same hold. Since $\sum_{i=1}^{|S|} \mu_r^\theta(i) = 1$ and $\sum_{i=1}^{|S|} \mu_s^\theta(i) = 1$, subtracting these two equations and rearranging yield

$$\mu_s^\theta(|S|) - \mu_r^\theta(|S|) = - \sum_{i=1}^{|S|-1} \left(\mu_s^\theta(i) - \mu_r^\theta(i) \right).$$

Applying Frobenius norm yields the desired result.

3. The boundedness of the average reward is immediate from part 2, i.e.,

$$\begin{aligned} \|\eta_s^\theta - \eta_r^\theta\|_F &= \left\| \mu_r^{\theta \top} r - \mu_s^{\theta \top} r \right\|_F \\ &\leq \left\| \mu_r^{\theta \top} - \mu_s^{\theta \top} \right\|_F \cdot \|r\|_F \\ &\leq B_\eta |S|. \end{aligned} \quad (31)$$

Similarly to part 2, the value function for sim and real are

$$\begin{aligned} \mathbf{v}_s^\theta &= r - \eta + P_s^\theta \mathbf{v}_s^\theta, \\ \mathbf{v}_r^\theta &= r - \eta + P_r^\theta \mathbf{v}_r^\theta. \end{aligned} \quad (32)$$

Subtracting both yields

$$\mathbf{v}_s^\theta - \mathbf{v}_r^\theta = P_s^\theta \mathbf{v}_s^\theta - P_r^\theta \mathbf{v}_r^\theta. \quad (33)$$

We add and subtract $P_s^\theta \mathbf{v}_r^\theta$ and rearrange to get

$$\begin{aligned} \mathbf{v}_s^\theta - \mathbf{v}_r^\theta &= P_s^\theta \mathbf{v}_s^\theta - P_s^\theta \mathbf{v}_r^\theta + P_s^\theta \mathbf{v}_r^\theta - P_r^\theta \mathbf{v}_r^\theta \\ \mathbf{v}_s^\theta - \mathbf{v}_r^\theta &= P_s^\theta (\mathbf{v}_s^\theta - \mathbf{v}_r^\theta) + (P_s^\theta - P_r^\theta) \mathbf{v}_r^\theta \\ (I - P_s^\theta) (\mathbf{v}_s^\theta - \mathbf{v}_r^\theta) &= (P_s^\theta - P_r^\theta) \mathbf{v}_r^\theta. \end{aligned} \quad (34)$$

Similarly to 2, we have an under-determined equation system. We assume that for both BEs of $\mathbf{v}_s^\theta(s^*) = \mathbf{v}_r^\theta(s^*) = 0$ in order for (32) to be each with a unique solution. Now, similarly to 2, we look at the $|S| - 1$ first equations (the now has a unique solution)

$$(\tilde{I} - \tilde{P}_s^\theta)(\tilde{\mathbf{v}}_s^\theta - \tilde{\mathbf{v}}_r^\theta) = (\tilde{P}_s^\theta - \tilde{P}_r^\theta)\tilde{\mathbf{v}}_r^\theta. \quad (35)$$

Again, similarly to 2 we get the desired result. □

B.2 Corollary for Theorem 4

The following corollary follows immediately from Theorem 4 and establishes that any convex combination of "close" enough sim and real share the same properties as both sim and real.

Corollary 7. *Assuming the same as in Theorem 4, if Y is a process where its dynamics can be described as $P_Y = \beta P_s(s'|s, a) + (1 - \beta)P_r(s'|s, a)$ for $0 \leq \beta \leq 1$, then Y satisfies the same properties as of Theorem 4 w.r.t. the real process.*

Proof. The process Y is a convex combination of both sim and real, therefore, the distance between P_r and P_Y is smaller than the distance between P_r and P_s . Using Theorem 4 the result follows immediately. □

C Experiment Details of Section 6

We trained the Fetch Push task using the DDPG algorithm [30] together with HER [1]. For DDPG, HER and FetchPush task we used the same hyper-parameters as in [1]. For completeness, we specify the hyper-parameters and task parameters used in our experiments.

C.1 Training procedure

We train for 150 epochs. Each epoch consists of 50 cycles where each cycle consists of running the policy for 2 episodes per worker. Every episode consists of 50 environment time-steps. Then, 40 optimization steps are performed on mini-batches of size 256 sampled uniformly from a replay buffer consisting of 10^6 transitions. For improved efficiency, the whole training procedure is distributed over 8 threads (workers) which average the parameters after every update. Training for 150 epochs took us approximately 2h using 8 cpu cores. The networks are optimized using the Adam optimizer [25] with learning rate of 0.001. We update the target networks after every cycle using the decay coefficient of 0.95. We use the discount factor of $\gamma = 0.98$ for all transitions and we clip the targets used to train the critic to the range of possible values, i.e. $[-\frac{1}{1-\gamma}, 0]$. The behavioral policy we use for exploration works as follows. With probability 0.3 we sample (uniformly) a random action from the hypercube of valid actions. Otherwise, we take the output of the policy network and add independently to every coordinate normal noise with standard deviation equal to 0.2 of the total range of allowed values on this coordinate. Goals selection for HER algorithm was performed using the "future" HER strategy with $k = 4$. See [1] for additional details.

C.2 Networks architecture

The architecture of the actor and critic networks is a Multi-Layer Perceptrons (MLP) with 3 hidden layers and ReLU activation function. Each layer has 256 hidden units. The actor output layer uses the tanh activation function and is rescaled so that it lies in the range $[-5\text{cm}, 5\text{cm}]$. We added the L_2 norm of the actions to the actor loss function to prevent tanh saturation and vanishing gradients (in the same way as in [1]). We rescale the inputs to the critic and actor networks so that they have mean zero and standard deviation equal to one and then clip them to the range $[-5, 5]$. Means and standard deviations used for rescaling are computed using all the observations encountered so far in the training.

C.3 Task parameters

The initial position of the gripper is fixed, located 20cm above the table. The initial position of the box on the table is randomized, in the $30\text{cm} \times 30\text{cm}$ square with the center directly under the

gripper. The width of the box is 5cm. The goal position is sampled uniformly from the same square as the box position.

The state space is 28-dimensional: 25 dimensions for the gripper and box poses and velocities and 3 for the goal position. The action space is 4-dimensional. Three dimensions specify the desired relative gripper position at the next time-step. The last dimension specifies the desired distance between the 2 fingers which are position controlled. Our task does not require gripper rotation and therefore we keep it fixed.

C.4 Friction values

In our experiments, the difference between the real and sim environments is the friction between the box and the table. The friction parameter is a vector of 5 dimensions: two tangential, one torsional, two rolling. In our experiments, the friction values in the real environment are $[0.03, 1., 0.005, 0.0001, 0.0001]$ and the friction values in the sim environment are $[2., 2., 0.005, 0.01, 0.0001]$. The sim friction values were chosen after a preceding experiment on the friction range $[1.8, 2.2] \times [1.8, 2.2] \times [0.005] \times [0.0001, 0.1] \times [0.0001, 0.1]$, respectively, which ensured that if we train a policy only on the simulator and use this policy in the real environment, it does not solve the task. In this way we have a simulator which is close to the real world, but not identical to it, what usually happens when designing simulators for real systems such as a robotic arm.

C.5 Performance evaluation

In our experiments, for each environment (real or sim) the task is solved if in the last time-step of an episode, the box position satisfies $\|\text{box position} - \text{goal position}\|_2 \leq 0.05$. After each training epoch, we tested in the *real* environment the trained policy for 10 episodes. The test was performed separately for each one of the 8 workers. For calculating the final success rate for each epoch we averaged the local success rate from each worker. Finally, for each q_r and β_r values, and for each mixing strategy, we repeated the experiment with 10 different random seeds.